International Journal of Engineering Science 98 (2016) 14–35

Contents lists available at ScienceDirect

International Journal of Engineering Science

journal homepage: www.elsevier.com/locate/ijengsci

Nonlinear effective behavior of a dispersion of randomly oriented coated ellipsoids with arbitrary temporal dispersion

Stefano Giordano*

Joint International Laboratory LIA LEMAC/LICS, Institute of Electronics, Microelectronic and Nanotechnology (UMR CNRS 8520), ComUE Lille Nord de France, Ecole Centrale de Lille, Avenue Poincaré, BP 60069, 59652 Villeneuve d'Ascq Cedex, France

ARTICLE INFO

Article history:
Received 27 May 2015
Revised 21 July 2015
Accepted 22 July 2015
Available online 12 August 2015

Keywords:
Random composite materials
Coated ellipsoidal particles
Homogenization
Hereditary constitutive equations
Temporal dispersion

ABSTRACT

This work deals with the determination of the linear and nonlinear effective properties of an heterogeneous material composed of a dispersion of coated ellipsoidal particles (core–shell structure). The particles are considered randomly oriented and positioned within the matrix. Moreover, all constitutive equations (matrix, cores, shells) exhibit an hereditary behavior, leading to an arbitrary temporal dispersion. While matrix and shell are considered linear, the particles core shows an additional third-order nonlinearity. We develop an effective medium theory, which allows us to calculate the linear and nonlinear response in terms of the microstructure features. In particular, we can investigate the effects of the inter-phase on the overall behavior, in combination with the randomness of the orientations and with the linear and nonlinear hereditary phenomena. The results may find relevant applications in material science and, more specifically, in nonlinear optics, bulk plasmonics and metamaterials.

1. Introduction

The elaboration of effective medium theories and homogenization procedures, useful to calculate the overall properties of heterogeneous materials, is an important topic with relevant applications in materials science and nano-technology. Indeed, several techniques have been successfully developed to analyse the electric, magnetic, thermal and elastic response of composite systems and complex structures (Milton, 2004; Torquato, 2002; Sahimi, 2003a; Sahimi, 2003b; Tartar, 2009; Kanaun & Levin, 2008a; Kanaun & Levin, 2008b; Sihvola, 1999).

From the historical point of view, Maxwell (1881) investigations represent the first analysis of the conductivity of a particulate systems composed of a dilute dispersion of spheres in a different matrix (see also the works of Maxwell-Garnett (1904), van Beek (1967) and Meredith (1959)). At a later stage, the dispersions of ellipsoids were considered by Fricke (1953) in order to model specific biological tissues. Furthermore, in order to study higher volume fractions of the dispersed phase, the differential method (Bruggeman, 1935; Norris, 1985; Giordano, 2003; Markov, Levin, Mousatov, & Kazatchenko, 2012; Markov, Mousatov, Kazatchenko, & Markova, 2014) and the multipole technique (Günther & Heinrich, 1965; Giordano, 2005a) have been introduced. Further developments have been elaborated by Myles, Peracchio, and Chiu (2014) and Myles, Peracchio, and Chiu (2015). Also, efficient numerical methods combined with theoretical analyses have been used by Kanaun (2010) and Kanaun (2011) to investigate the properties of heterogeneous structures. From the point of view of the

* Tel.: +33 (0) 3 20 19 79 58; fax: +33 (0) 3 20 19 79 84.
E-mail address: Stefano.Giordano@iemn.univ-lille1.fr

http://dx.doi.org/10.1016/j.ijengsci.2015.07.009
0020-7225/

mechanical homogenization theories, the classical starting point is the Eshelby (1957) property describing the elastic fields generated by an ellipsoidal inhomogeneity. This result has been largely used to obtain the elastic properties of particulate composites (Giordano, 2005b; Kachanov & Sevostianov, 2005), multi-grained materials (Kröner, 1978; Giordano, 2007) and multi-cracked systems (Kachanov, 1994; Giordano & Colombo, 2007; Kanaun & Levin, 2009; Kanaun & Markov, 2014).

An interesting approach, based on the equivalent inclusion method, i.e. on the original Eshelby (1957) idea, has been developed in the framework of the steady-state thermal conduction (Hatta & Taya, 1985; Hatta & Taya, 1986a; Hatta & Taya, 1986b). Moreover, the physical characterization of several complex materials has been performed by means of the so-called depolarization tensor (Weiglhofer, Lakhtakia, & Michel, 1997; Lakhtakia & Weiglhofer, 2000; Mackay, 2011), which represents the analogous of the Eshelby tensor, applied to the electromagnetic or transport properties. More recently, a fully anisotropic analysis has been conducted for ellipsoidal particles (Giordano & Palla, 2008) and for parallel or random dispersions of cracks in conductive systems (Giordano & Palla, 2012). Also, anisotropic multi-layered systems have been thoroughly analysed through the homogenization methodology and several analytical exact results have been found for the magneto-electro-elastic coupling (Kim, 2011; Giordano, 2014; Giordano et al., 2014).

The nonlinear case has been largely analysed since it concerns properties of great importance for describing real situations. Indeed, such investigations find relevant applications in nonlinear optics (Mills, 1991; Goncharenko, Popelnukh, & Venger, 2002; Goncharenko, 2004; Goncharenko, 2007; Boyd, 2008), in the intrinsic optical bistability (Bergman, Levy, & Stroud, 1994; Pinchuk, 2003), in the second and third harmonic generation (Hui, Cheung, & Stroud, 1998), in the recently developed nonlinear plasmonics (Kauranen & Zayats, 2012; Furtado & Gómez-Malagón, 2014) and in metamaterials (Lapine, Shadrivov, & Kivshar, 2014). Homogenization techniques have been therefore proposed for populations of nonlinear particles embedded in a linear matrix (Lakhtakia & Weiglhofer, 2000; Giordano & Rocchia, 2005; Giordano & Rocchia, 2006). The mechanical characterization of nonlinear nanocomposites has been considered as well, see e.g. the works by Colombo and Giordano (2011), by Guerder, Giordano, Bou Matar, and Vasseur (2015) and references therein.

A crucial point that should be carefully considered in any effective medium theory concerns the presence of imperfect interfaces between the constituents of composite materials. Indeed, in many real cases of technological interest (especially at the nanoscale), the specific properties of real interfaces play a important role in determining the effective transport properties, being e.g. at the origin of the scale effects. In related literature two interface models have been proposed and largely used for describing two different limiting situations. The first zero thickness model is called *low conducting interface* and it is based on the so-called Kapitza (1964) resistance. Conversely, the second model, called *high conducting interface*, concerns the case of an interphase of very high conductivity with vanishing thickness. Several investigations have been devoted to understand the response of heterogeneous materials with low conducting interfaces (Benveniste & Miloh, 1986; Benveniste, 1987; Hasselman & Johnson, 1987; Torquato & Rintoul, 1995; Lipton & Vernescu, 1996; Nan, Birringer, Clarke, & Gleiter, 1997; Hashin, 2001; Duan & Karihaloo, 2007; Le Quang, He, & Bonnet, 2011; Le Quang, Pham, Bonnet, & He, 2013) or with high conducting interfaces (Torquato & Rintoul, 1995; Duan & Karihaloo, 2007; Le Quang, Bonnet, & He, 2010; Le Quang et al., 2013; Lipton, 1997; Miloh & Benveniste, 1999). Recent results concern the integration of the low and high interface paradigms in more general models based on the T and Π lattice structures (Pavanello, Manca, Palla, & Giordano, 2012; Pavanello & Giordano, 2013), theories for composites with curvilinearly anisotropic coated inclusions (Benveniste, 2013), the prediction of transport behaviors in aggregates with soft interfacial layers (Xu, Chen, Chen, & Jiang, 2014) and the interphase description within the two-temperature model (Giordano & Manca, 2014).

In this work we develop an homogenization theory able to combine three specific aspects, separately considered in several of the above discussed investigations, namely: (i) the randomness of the orientations in a population of ellipsoidal particles embedded in a given matrix; (ii) the presence of a coating (or finite-thickness inter-phase or shell) between the core of each particle and the matrix (it can model all the intermediate cases between the low and the high conducting interface models); (iii) the specific constitutive equations of matrix, shells and cores, exhibiting an hereditary behavior leading to an arbitrary temporal dispersion; while matrix and shell are considered linear, the particles core shows an additional third-order nonlinearity. The entire development is presented for the dielectric behavior of the involved materials (described by their permittivities and nonlinear susceptibilities). However, it is well known that the solutions can be used to describe similar situations concerning the magnetic behavior of the composite material and the transport properties (diffusion, electric and thermal conduction), as well.

2. Problem statement

In this Section we introduce the structure analysed in this paper and, in particular, the constitutive equations adopted to describe the involved materials. The geometry is represented in Fig. 1, where one can find a dispersion of randomly oriented coated particles. The coated assemblage is characterized by two confocal ellipsoids, hence generating an internal core and a different external shell for each particle. Then, all particles are embedded in a third material, the matrix of the composite structure. This heterogeneous microstructure, as discussed in the Introduction, is largely used in material science and, more specifically, in nonlinear optics, bulk plasmonics and metamaterials. In the following, we define the constitutive equations of the three phases.

In particular, we will consider matrix and shell described by a linear isotropic response which includes a temporal dispersion, as follows

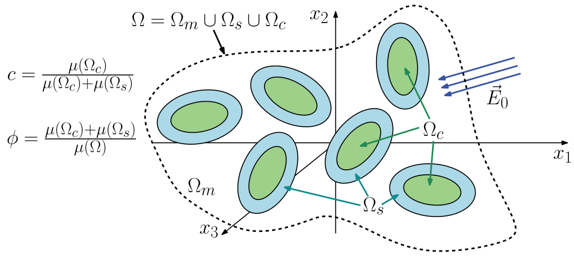

Fig. 1. Dispersion of randomly oriented composite particles embedded in a different homogeneous matrix.

$$\vec{D}(\vec{x},t) = \int_0^{+\infty} g(\tau)\,\vec{E}(\vec{x},t-\tau)d\tau, \tag{1}$$

where $g(\tau)$ is a known function representing the hereditary effects between the electric field and the electric displacement vectors (Landau, Pitaevskii, & Lifshitz, 1984; Boyd, 2008). If we are interested in the sinusoidal steady state described by monochromatic fields, we impose $\vec{E}(\vec{x},t) = \Re e\{\dot{\vec{E}}(\vec{x},\omega)e^{i\omega t}\}$, where $\dot{\vec{E}}(\vec{x},\omega)$ is the phasor vector corresponding to the frequency ω. Accordingly, we will have a displacement vector given by the similar expression $\vec{D}(\vec{x},t) = \Re e\{\dot{\vec{D}}(\vec{x},\omega)e^{i\omega t}\}$. The two field and displacement phasors are therefore connected through the important relationship

$$\dot{\vec{D}}(\vec{x},\omega) = \dot{\varepsilon}(\omega)\dot{\vec{E}}(\vec{x},\omega), \tag{2}$$

where $\dot{\varepsilon}(\omega)$ represents the (causal or one-sided) Fourier transform of $g(\tau)$

$$\dot{\varepsilon}(\omega) = \int_0^{+\infty} g(\tau)e^{-i\omega\tau}d\tau. \tag{3}$$

This form of constitutive equation will be adopted for the shell and the matrix. It means that they will be described by the complex valued permittivities $\dot{\varepsilon}_2(\omega)$ and $\dot{\varepsilon}_1(\omega)$, respectively (corresponding to different hereditary kernels $g_2(\tau)$ and $g_1(\tau)$).

Concerning the core of the particles, we will adopt again an isotropic response with temporal dispersion but we introduce a further nonlinear behavior (Kerr-like), as follows

$$\vec{D}_c(\vec{x},t) = \int_0^{+\infty} f(\tau)\vec{E}_c(\vec{x},t-\tau)d\tau + \int_0^{+\infty}\int_0^{+\infty} \vartheta(\tau_1,\tau_2)\,\|\vec{E}_c(\vec{x},t-\tau_1)\|^2\vec{E}_c(\vec{x},t-\tau_2)d\tau_1 d\tau_2, \tag{4}$$

where $f(\tau)$ describes a linear hereditary term, as previously discussed, and $\vartheta(\tau_1,\tau_2)$ represents the most general isotropic nonlinear response, expanded up to the third order in the electric field. Since we are interested in an isotropic response, the second order term of nonlinearity has been omitted. Moreover, always for the isotropy hypothesis, the hereditary mechanism is based on two time lags τ_1 and τ_2, related to $\|\vec{E}_c(\vec{x},t-\tau_1)\|^2$ and $\vec{E}_c(\vec{x},t-\tau_2)$, respectively. The complete response described by Eq. (4) is very complicated and, in particular, characterizes the third harmonic generation, creating a complex spectrum for the involved fields. However, we are here interested in the sinusoidal steady state at frequency ω. Therefore, we can consider an electric field $\vec{E}_c(\vec{x},t) = \Re e\{\dot{\vec{E}}_c(\vec{x},\omega)e^{i\omega t}\}$ as input of Eq. (4). Accordingly, we may determine the exact response for the electric displacement. In this result, we retain all terms at frequency ω and we neglect the others. After a very long but straightforward calculation, we can prove that the phasor of the electric displacement $\dot{\vec{D}}_c(\vec{x},\omega)$ at frequency ω can be written as

$$\begin{aligned}\dot{\vec{D}}_c(\vec{x},\omega) = {} & \dot{\varepsilon}_3(\omega)\dot{\vec{E}}_c(\vec{x},\omega) + \frac{1}{2}\dot{\chi}(0,\omega)\left[\dot{\vec{E}}_c(\vec{x},\omega)\cdot\dot{\vec{E}}_c^{*}(\vec{x},\omega)\right]\dot{\vec{E}}_c(\vec{x},\omega)\\ & + \frac{1}{4}\dot{\chi}(2\omega,\omega)\left[\dot{\vec{E}}_c(\vec{x},\omega)\cdot\dot{\vec{E}}_c(\vec{x},\omega)\right]\dot{\vec{E}}_c^{*}(\vec{x},\omega),\end{aligned} \tag{5}$$

where

$$\dot{\varepsilon}_3(\omega) = \int_0^{+\infty} f(\tau)e^{-i\omega\tau}d\tau, \tag{6}$$

similarly to Eq. (3), and

$$\dot{\chi}(\omega_1,\omega_2) = \int_0^{+\infty}\int_0^{+\infty} \vartheta(\tau_1,\tau_2)e^{-i(\omega_1\tau_1+\omega_2\tau_2)}d\tau_1 d\tau_2 \tag{7}$$

is the two-dimensional Fourier transform of the function $\vartheta(\tau_1, \tau_2)$. We remark that Eq. (5) is not mathematically equivalent to Eq. (4) since it only represents the behavior of the first harmonic at frequency ω. The presence of the couple of the third order terms $[\dot{\vec{E}}_c(\vec{x},\omega)\cdot\dot{\vec{E}}_c^*(\vec{x},\omega)]\dot{\vec{E}}_c(\vec{x},\omega)$ and $[\dot{\vec{E}}_c(\vec{x},\omega)\cdot\dot{\vec{E}}_c(\vec{x},\omega)]\dot{\vec{E}}_c^*(\vec{x},\omega)$ is a classical result for hereditary nonlinear constitutive equations, well known in nonlinear optics (Landau et al., 1984; Mills, 1991; Boyd, 2008). Therefore, in terms of phasors, we have a nonlinear relation between $\dot{\vec{E}}_c(\vec{x},\omega)$ and $\dot{\vec{D}}_c(\vec{x},\omega)$ that can be summed up through an electric field dependent permittivity tensor defined by

$$\dot{\hat{\varepsilon}}_{3,tot}(\omega) = \dot{\hat{\varepsilon}}_3(\omega) + \frac{1}{2}\dot{\chi}_1(\omega)\dot{\vec{E}}_c(\vec{x},\omega)\cdot\dot{\vec{E}}_c^*(\vec{x},\omega)\hat{I} + \frac{1}{4}\dot{\chi}_2(\omega)\dot{\vec{E}}_c^*(\vec{x},\omega)\otimes\dot{\vec{E}}_c(\vec{x},\omega), \tag{8}$$

where, for convenience, we introduced $\dot{\chi}_1(\omega) = \dot{\chi}(0,\omega)$ and $\dot{\chi}_2(\omega) = \dot{\chi}(2\omega,\omega)$, representing two frequency-dependent nonlinear susceptibilities. In Eq. (8) we used the tensor product of vectors defined as follows: if $\hat{C} = \vec{A}\otimes\vec{B}$, then we have $T_{ij} = A_i B_j$.

A particular case, important for many practical applications, concerns the situation where the two time lags τ_1 and τ_2 are coincident in Eq. (4). It means that the $\vartheta(\tau_1, \tau_2) = \delta(\tau_1 - \tau_2)\lambda(\tau_1)$ and Eq. (4) assumes the simplified form

$$\begin{aligned}\vec{D}_c(\vec{x},t) = &\int_0^{+\infty} f(\tau)\vec{E}_c(\vec{x},t-\tau)d\tau \\ &+ \int_0^{+\infty}\lambda(\tau)\parallel\vec{E}_c(\vec{x},t-\tau)\parallel^2\vec{E}_c(\vec{x},t-\tau)d\tau.\end{aligned} \tag{9}$$

It is not difficult to prove that, in this case, we have $\dot{\chi}(0,\omega) = \dot{\chi}(2\omega,\omega)$ or, equivalently, $\dot{\chi}_1(\omega) = \dot{\chi}_2(\omega)$. Hence, we can write the frequency-dependent permittivity tensor as follows

$$\dot{\hat{\varepsilon}}_{3,tot}(\omega) = \dot{\hat{\varepsilon}}_3(\omega) + \dot{\chi}_1(\omega)\left[\frac{1}{2}\dot{\vec{E}}_c(\vec{x},\omega)\cdot\dot{\vec{E}}_c^*(\vec{x},\omega)\hat{I} + \frac{1}{4}\dot{\vec{E}}_c^*(\vec{x},\omega)\otimes\dot{\vec{E}}_c(\vec{x},\omega)\right], \tag{10}$$

where a single susceptibility $\dot{\chi}_1(\omega)$ is able to describe the whole response at frequency ω.

It is interesting to observe that, although the dispersion behavior of the particle cores is isotropic, the equivalent permittivity tensor in the frequency domain is effectively anisotropic, with the general form given in Eq. (8). This point explains why we will consider an anisotropic core in the first part of the present paper.

3. The coated ellipsoid geometry

We consider here a single coated ellipsoidal particle composed of core and shell embedded in a matrix (see Fig. 2 for details). To begin, we suppose that the three materials are linear without temporal dispersion and we assume an arbitrary anisotropy for the core (with permittivity tensor $\hat{\varepsilon}_3$), while shell and matrix are considered isotropic (with scalar permittivity ε_2 and ε_1, respectively). The ellipsoidal interfaces are supposed to be confocal, so that we can write the equation

$$\sum_{i=1}^{3}\frac{x_i^2}{a_{s,i}^2+\xi} = 1, \tag{11}$$

where $\xi = 0$ corresponds to the interface between shell and matrix and $\xi = \xi_c < 0$ corresponds to the interface between core and shell. Therefore, in Eq. (11) the points with $\xi > 0$ are external to the particle and those with $\xi < 0$ belong to the particle itself. The lengths $a_{s,i}$ represent the semiaxes of the external shell interface and $a_{c,i} = \sqrt{a_{s,i}^2 + \xi_c}$ the semiaxes of the core interface. For the sake of definiteness, we can impose $0 < a_{s,3} < a_{s,2} < a_{s,1} < +\infty$, so that we have the natural limitation $\xi > -a_{s3}^2$. We suppose now to apply a uniform electric field $\vec{E}_0$ (arbitrarily oriented in the space) to the structure above described. It means that $\vec{E}_0$ is the electric field pre-existing before the introduction of the particle into the linear isotropic and homogeneous space ε_1. We are interested in determining the perturbation of the electric potential induced by the coated

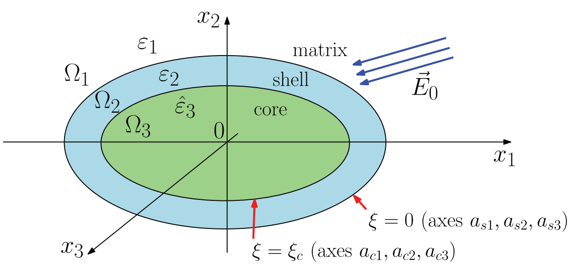

Fig. 2. Confocal structure corresponding to the composite particle composed of a core and a shell embedded in an external matrix.

particle. We suppose that the perturbed electric field in each region of our structure (core, shell and matrix) can be represented by the following expressions

$$\phi_c = \vec{C} \cdot \vec{x}, \tag{12}$$

$$\phi_s = \vec{S} \cdot \vec{x} + \vec{T} \cdot \vec{F}(\vec{x}), \tag{13}$$

$$\phi_m = -\vec{E}_0 \cdot \vec{x} + \vec{Q} \cdot \vec{F}(\vec{x}), \tag{14}$$

where $\vec{C}$, $\vec{S}$, $\vec{T}$ and $\vec{Q}$ are vectors to be determined by imposing the pertinent boundary conditions (see below for details). Moreover, the function $\vec{F}(\vec{x})$ is defined through its components as

$$\left[\vec{F}(\vec{x})\right]_k = x_k \int_{\xi}^{+\infty} \frac{dt}{R(t)\left(a_{s,k}^2 + t\right)}, \tag{15}$$

where we used the following definition

$$R(t) = \sqrt{\prod_{i=1}^{3}\left(a_{s,i}^2 + t\right)}, \tag{16}$$

and where ξ must be obtained as solution of Eq. (11) with fixed x_1, x_2 and x_3 ($\xi > -a_{s,3}^2$).

Typically, for analysing the behavior of confocal isotropic geometries, the the ellipsoidal coordinates and the Lamé functions (or ellipsoidal harmonic functions related to the separation of variables applied to the Laplace equation in elliptic coordinates) strongly simplify the mathematical derivations (Benveniste & Miloh, 1991). However, in our case we are forced to use Cartesian variables because of the anisotropic behavior of the particles core. Indeed, the separation of variables for the anisotropic Laplace equations leads to more complicated differential equations, whose solutions can not be directly written in terms of standard Lamé functions.

Now, we specify on each interface the boundary conditions imposing the continuity of the electrical potential and the continuity of the normal component of the electric displacement. These conditions represent the ideal behavior of the fields at an interface without imperfections. We can assume such conditions since the imperfect character of the transport process between core and matrix is taken into account through the presence of the shell, which represents a finite-thickness inter-phase mimicking the possible contact defects. However, it is important to remark that the thickness of the coating (shell) with confocal ellipsoidal boundaries is not constant and it varies changing the point considered over the surface. Therefore, the introduction of imperfect interfaces through this variable layer is an approximation, which is more acceptable when particles are nearly spherical (Kushch, Sevostianov, & Belyaev, 2015).

Explicitly, we obtain

$$\phi_c = \phi_s \quad if \quad \xi = \xi_c, \tag{17}$$

$$\phi_s = \phi_m \quad if \quad \xi = 0, \tag{18}$$

$$\sum_j \sum_i \varepsilon_{3,ij} \frac{\partial \phi_c}{\partial x_i} n_j = \varepsilon_2 \sum_j \frac{\partial \phi_s}{\partial x_j} n_j \quad if \quad \xi = \xi_c, \tag{19}$$

$$\varepsilon_2 \sum_j \frac{\partial \phi_s}{\partial x_j} n_j = \varepsilon_1 \sum_j \frac{\partial \phi_m}{\partial x_j} n_j \quad if \quad \xi = 0, \tag{20}$$

where $\vec{n} = (n_1, n_2, n_3)$ is the outward normal unit vector to each surface. By using Eqs. (12) and (13) the first boundary condition can be rewritten as

$$\sum_k C_k x_k = \sum_k S_k x_k + \sum_k T_k x_k \int_{\xi_c}^{+\infty} \frac{dt}{R(t)\left(a_{s,k}^2 + t\right)}. \tag{21}$$

The integral in the above equality can be elaborated by using the change of variable $\eta = t - \xi_c$. The result is

$$\sum_k C_k x_k = \sum_k S_k x_k + \frac{2}{A_c} \sum_k T_k x_k L_{ck}, \tag{22}$$

where $A_c \triangleq R(\xi_c) = a_{c1} a_{c2} a_{c3}$ and we introduced the depolarization factors of the core (Landau et al., 1984)

$$L_{ck} \triangleq \frac{A_c}{2} \int_0^{+\infty} \frac{d\eta}{\sqrt{\prod_{i=1}^{3}\left(a_{c,i}^2 + \eta\right)}\left(a_{c,k}^2 + \eta\right)}. \tag{23}$$

In we take into account the arbitrariness of the point (x_1, x_2, x_3) on the core–shell interface in Eq. (22), we obtain the explicit form of the first boundary condition

$$C_k = S_k + \frac{2}{A_c} T_k L_{ck}, \forall k = 1, 2, 3. \tag{24}$$

The second one can be elaborated in a similar manner. By substituting Eqs. (13) and (14) in Eq. (18) we eventually obtain

$$\sum_k S_k x_k + \frac{2}{A_s} \sum_k T_k x_k L_{sk} = -\sum_k E_{0k} x_k + \frac{2}{A_s} \sum_k Q_k x_k L_{sk}, \tag{25}$$

where, as before, we defined $A_s \triangleq R(0) = a_{s1} a_{s2} a_{s3}$ and we introduced the depolarization factors of the shell (Landau et al., 1984)

$$L_{sk} \triangleq \frac{A_s}{2} \int_0^{+\infty} \frac{d\eta}{\sqrt{\prod_{i=1}^3 \left(a_{s,i}^2 + \eta\right)} \left(a_{s,k}^2 + \eta\right)}. \tag{26}$$

From Eq. (25) we finally deduce that

$$S_k + \frac{2}{A_s} T_k L_{sk} = -E_{0k} + \frac{2}{A_s} Q_k L_{sk}, \forall k = 1, 2, 3. \tag{27}$$

The elaboration of the third boundary condition is a more complicated task because of the presence of the term $\partial\phi_s/\partial x_j$. To begin we easily obtain

$$\frac{\partial \phi_s}{\partial x_j} = S_j + \sum_k \left[T_k \delta_{kj} \int_\xi^{+\infty} \frac{dt}{R(t)\left(a_{s,k}^2 + t\right)} + T_k x_k \frac{\partial}{\partial x_j} \int_\xi^{+\infty} \frac{dt}{R(t)\left(a_{s,k}^2 + t\right)} \right], \tag{28}$$

and we determine the last integral as follows

$$\frac{\partial}{\partial x_j} \int_\xi^{+\infty} \frac{dt}{R(t)\left(a_{s,k}^2 + t\right)} = \frac{d}{d\xi} \int_\xi^{+\infty} \frac{dt}{R(t)\left(a_{s,k}^2 + t\right)} \frac{\partial \xi}{\partial x_j} = -\frac{1}{R(\xi)\left(a_{s,k}^2 + \xi\right)} \frac{\partial \xi}{\partial x_j}. \tag{29}$$

Now, to calculate $\frac{\partial \xi}{\partial x_j}$ we define

$$f(x_1, x_2, x_2, \xi) = \sum_{i=1}^{3} \frac{x_i^2}{a_{s,i}^2 + \xi} - 1. \tag{30}$$

Since the value of ξ as function of x_1, x_2 and x_3 is defined by $f = 0$, we also have

$$\frac{\partial f}{\partial x_j} + \frac{\partial f}{\partial \xi} \frac{\partial \xi}{\partial x_j} = 0 \Rightarrow \frac{\partial \xi}{\partial x_j} = -\frac{\frac{\partial f}{\partial x_j}}{\frac{\partial f}{\partial \xi}} = \frac{2x_j}{a_{s,j}^2 + \xi} \frac{1}{\sum_q \frac{x_q^2}{\left(a_{s,q}^2 + \xi\right)^2}}. \tag{31}$$

Summing up, Eq. (28) becomes

$$\frac{\partial \phi_s}{\partial x_j} = S_j + \sum_k \left[T_k \delta_{kj} \int_\xi^{+\infty} \frac{dt}{R(t)\left(a_{s,k}^2 + t\right)} - \frac{2x_k x_j T_k}{R(\xi)\left(a_{s,k}^2 + \xi\right)\left(a_{s,j}^2 + \xi\right)} \frac{1}{\sum_q \frac{x_q^2}{\left(a_{s,q}^2 + \xi\right)^2}} \right], \tag{32}$$

and the boundary condition in Eq. (19) assumes the form

$$\begin{aligned} \sum_{ij} \varepsilon_{3,ij} C_i n_j &= \varepsilon_2 \sum_j S_j n_j \\ &\quad + \varepsilon_2 \sum_{kj} \left[T_k \delta_{kj} n_j \int_{\xi_c}^{+\infty} \frac{dt}{R(t)\left(a_{s,k}^2 + t\right)} - \frac{2x_k x_j T_k n_j}{R(\xi_c)\left(a_{s,k}^2 + \xi_c\right)\left(a_{s,j}^2 + \xi_c\right)} \frac{1}{\sum_q \frac{x_q^2}{\left(a_{s,q}^2 + \xi_c\right)^2}} \right] \\ &= \varepsilon_2 \sum_j S_j n_j + \varepsilon_2 \sum_j T_j n_j \int_{\xi_c}^{+\infty} \frac{dt}{R(t)\left(a_{s,k}^2 + t\right)} - \varepsilon_2 \sum_{kj} \frac{2x_k x_j T_k n_j}{R(\xi_c) a_{c,k}^2 a_{c,j}^2} \frac{1}{\sum_q \frac{x_q^2}{a_{c,q}^4}}, \end{aligned} \tag{33}$$

where we used the definition $a_{c,k}^2 = a_{s,k}^2 + \xi_c$. In the last term we consider the following theorem concerning the outward normal unit vector to an ellipsoid (in this case the core–shell interface), which is proved in Appendix A

$$n_k = \frac{x_k}{a_{c,k}^2} \sum_j \frac{x_j n_j}{a_{c,j}^2} / \sum_q \frac{x_q^2}{a_{c,q}^4} \quad (\forall\ k = 1, 2, 3), \tag{34}$$

and, we therefore obtain from Eq. (19)

$$\sum_{ij} \varepsilon_{3,ij} C_i n_j = \varepsilon_2 \sum_j S_j n_j + \frac{2}{A_c} \varepsilon_2 \sum_j T_j L_{cj} n_j - \frac{2}{A_c} \varepsilon_2 \sum_k T_k n_k, \tag{35}$$

or, equivalently, for the arbitrariness of $\vec{n}$,

$$\sum_i \varepsilon_{3,ij} C_i = \varepsilon_2 S_j + \frac{2}{A_c} \varepsilon_2 T_j L_{cj} - \frac{2}{A_c} \varepsilon_2 T_j. \tag{36}$$

We can similarly elaborate the fourth boundary condition. Following the previous procedure, Eq. (20) can be rewritten in the following form

$$\varepsilon_2 \sum_j \left[S_j + \sum_k T_k \delta_{kj} \frac{2}{A_s} L_{sk} - \sum_k \frac{2 x_k x_j T_k}{R(0) a_{s,k}^2 a_{s,j}^2} \frac{1}{\sum_q \frac{x_q^2}{a_{s,q}^4}} \right] n_j = \varepsilon_1 \sum_j \left[-E_{0j} + \sum_k Q_k \delta_{kj} \frac{2}{A_s} L_{sk} - \sum_k \frac{2 x_k x_j Q_k}{R(0) a_{s,k}^2 a_{s,j}^2} \frac{1}{\sum_q \frac{x_q^2}{a_{s,q}^4}} \right] n_j. \tag{37}$$

Then we can use the theorem stated in Appendix A for the shell-matrix ellipsoidal interface

$$n_k = \frac{x_k}{a_{s,k}^2} \sum_j \frac{x_j n_j}{a_{s,j}^2} \Bigg/ \sum_q \frac{x_q^2}{a_{s,q}^4} \quad (\forall\ k = 1, 2, 3), \tag{38}$$

in both the left and right hand sides of Eq. (37). The result has been eventually found as

$$\varepsilon_2 S_k + \varepsilon_2 \frac{2}{A_s} T_k L_{sk} - \varepsilon_2 \frac{2}{A_s} T_k = -\varepsilon_1 E_{0k} S_k + \varepsilon_1 \frac{2}{A_s} Q_k L_{sk} - \varepsilon_1 \frac{2}{A_s} Q_k, \tag{39}$$

concluding the analysis of the boundary conditions. To sum up, we can rewrite the four boundary conditions obtained in Eqs. (24), (27), (36) and (39) in vector form as follows

$$\vec{C} = \vec{S} + \frac{2}{A_c} \hat{L}_c \vec{T}, \tag{40}$$

$$\vec{S} + \frac{2}{A_s} \hat{L}_s \vec{T} = -\vec{E}_0 + \frac{2}{A_s} \hat{L}_s \vec{Q}, \tag{41}$$

$$\hat{\varepsilon}_3 \vec{C} = \varepsilon_2 \left[\vec{S} + \frac{2}{A_c} \left(\hat{L}_c - \hat{I} \right) \vec{T} \right], \tag{42}$$

$$\varepsilon_2 \left[\vec{S} + \frac{2}{A_s} \left(\hat{L}_s - \hat{I} \right) \vec{T} \right] = \varepsilon_1 \left[-\vec{E}_0 + \frac{2}{A_s} \left(\hat{L}_s - \hat{I} \right) \vec{Q} \right], \tag{43}$$

where we defined $\hat{L}_c = \mathrm{diag}(L_{c1}, L_{c2}, L_{c3})$ and $\hat{L}_s = \mathrm{diag}(L_{s1}, L_{s2}, L_{s3})$. After a very long but straightforward algebraic development, we can obtain the solution of Eqs. (40)–(43) as follows

$$\vec{T} = -\frac{1}{2} \varepsilon_1 A_s A_c \left(\hat{\varepsilon}_3 - \varepsilon_2 \hat{I} \right) \hat{D}^{-1} \vec{E}_0, \tag{44}$$

$$\vec{S} = \varepsilon_1 A_s \left[\varepsilon_2 \hat{I} + \hat{L}_c \left(\hat{\varepsilon}_3 - \varepsilon_2 \hat{I} \right) \right] \hat{D}^{-1} \vec{E}_0, \tag{45}$$

$$\vec{C} = \varepsilon_1 \varepsilon_2 A_s \hat{D}^{-1} \vec{E}_0, \tag{46}$$

$$\vec{Q} = \frac{1}{2} A_s \hat{N} \hat{D}^{-1} \vec{E}_0, \tag{47}$$

where, to compact the final expressions, we defined the tensors $\hat{N}$ and $\hat{D}$

$$\begin{aligned} \hat{N} = & A_c \left[\hat{L}_s (\varepsilon_2 - \varepsilon_1) - \varepsilon_2 \hat{I} \right] \left(\hat{\varepsilon}_3 - \varepsilon_2 \hat{I} \right) \\ & - A_s (\varepsilon_2 - \varepsilon_1) \left[\varepsilon_2 \hat{I} + \hat{L}_c \left(\hat{\varepsilon}_3 - \varepsilon_2 \hat{I} \right) \right], \end{aligned} \tag{48}$$

$$\begin{aligned} \hat{D} = & A_c (\varepsilon_2 - \varepsilon_1) \hat{L}_s \left(\hat{L}_s - \hat{I} \right) \left(\hat{\varepsilon}_3 - \varepsilon_2 \hat{I} \right) \\ & - A_s \left[\varepsilon_1 \hat{I} + \hat{L}_s (\varepsilon_2 - \varepsilon_1) \right] \left[\varepsilon_2 \hat{I} + \hat{L}_c \left(\hat{\varepsilon}_3 - \varepsilon_2 \hat{I} \right) \right]. \end{aligned} \tag{49}$$

This completes the static analysis of the behavior of a coated particle with confocal ellipsoidal interfaces and anisotropic core. It is noteworthy that, in spite of the complex analytical procedure above discussed, we obtained simple results in algebraic form, merely depending on the depolarization factors of both ellipsoidal interfaces. We underline that the electric field induced within the core, assuming the value $-\vec{C}$ as deduced from Eq. (12), is always uniform in spite of the presence of the shell. As a particular case, we can take into consideration a particle without shell (homogeneous particle). To do this, we can impose $\hat{L}_c = \hat{L}_s$ and $A_c = A_s$ (the core coincide with the whole particle and the shell disappears), by getting the following results

$$\vec{C}_{hom} = -\varepsilon_1\left[\varepsilon_1\hat{I} + \hat{L}_s\left(\hat{\varepsilon}_3 - \varepsilon_1\hat{I}\right)\right]^{-1}\vec{E}_0, \tag{50}$$

$$\vec{Q}_{hom} = \frac{1}{2}A_s\left(\hat{\varepsilon}_3 - \varepsilon_1\hat{I}\right)\left[\varepsilon_1\hat{I} + \hat{L}_s\left(\hat{\varepsilon}_3 - \varepsilon_1\hat{I}\right)\right]^{-1}\vec{E}_0. \tag{51}$$

While $-\vec{C}_{hom}$ represents the internal field within the homogeneous particle, $\vec{Q}_{hom}$ describes the behavior of the external field in the same case. We remark that, performing the limit $\hat{L}_c \to \hat{L}_s$ and $A_c \to A_s$ we obtained, as expected, results not depending on ε_2, representing the permittivity of the shell, certainly not relevant for the homogeneous particle (with response $\hat{\varepsilon}_3$). Results given in Eqs. (50) and (51) are in perfect agreement with previous literature (Fricke, 1953; Landau et al., 1984; Giordano, 2003; Giordano, Palla, & Colombo, 2008). In this context, Eq. (51) is useful to determine an effective permittivity tensor $\hat{\varepsilon}_{eff}$pertinent to the composite (core–shell) particle. As a matter of fact, we can define an homogeneous equivalent particle by imposing exactly the same external electric potential generated by the effective particle and the composite one. More explicitly, $\hat{\varepsilon}_{eff}$must be calculated by imposing that $\vec{Q}_{hom} = \vec{Q}$ where in $\vec{Q}_{hom}$ we substitute $\hat{\varepsilon}_3 = \hat{\varepsilon}_{eff}$ and $\vec{Q}$ is given by Eq. (47). More explicitly, $\hat{\varepsilon}_{eff}$ is solution of the operator equation $(\hat{\varepsilon}_{eff} - \varepsilon_1\hat{I})[\varepsilon_1\hat{I} + \hat{L}_s(\hat{\varepsilon}_{eff} - \varepsilon_1\hat{I})]^{-1} = \hat{N}\hat{D}^{-1}$, which allows us to obtain

$$\begin{aligned}\hat{\varepsilon}_{eff} &= \varepsilon_1\left[\hat{I} - \hat{N}\hat{D}^{-1}\hat{L}_s\right]^{-1}\left[\hat{I} - \hat{N}\hat{D}^{-1}\left(\hat{L}_s - \hat{I}\right)\right] \\ &= \varepsilon_1\hat{I} + \varepsilon_1\hat{N}\left[\hat{D} - \hat{L}_s\hat{N}\right]^{-1},\end{aligned} \tag{52}$$

where $\hat{N}$ and $\hat{D}$ are defined in Eqs. (48) and (49), respectively. In order to prove the coherence of this result, we must verify that $\hat{\varepsilon}_{eff}$ is independent of ε_1, a parameter pertinent to the matrix. Indeed, we will obtain $\hat{\varepsilon}_{eff}$ as function of $c = A_c/A_s$ (volume fraction of the core within the shell), ε_2 and $\hat{\varepsilon}_3$. To do this, we can substitute Eqs. (48) and (49) in Eq. (52) and, after a long calculation, we obtain $\hat{\varepsilon}_{eff}$ in explicit form as follows

$$\hat{\varepsilon}_{eff} = \varepsilon_2\hat{I} - c\varepsilon_2\left(\hat{\varepsilon}_3 - \varepsilon_2\hat{I}\right)\left[\left(c\hat{L}_s - \hat{L}_c\right)\left(\hat{\varepsilon}_3 - \varepsilon_2\hat{I}\right) - \varepsilon_2\hat{I}\right]^{-1}. \tag{53}$$

We remark that for $c = 0$ we obtain $\hat{\varepsilon}_{eff} = \varepsilon_2\hat{I}$ and for $c = 1$ (and $\hat{L}_s = \hat{L}_c$) we have $\hat{\varepsilon}_{eff} = \hat{\varepsilon}_3$, as expected.

For the following purposes, we need to know the average value of the electric field within the shell region. This point will be useful to perform the averaging of the electric field in a more complex structure with a population of particles. To approach this problem we firstly prove the following property: the average field inside the composite particle composed of a core $\hat{\varepsilon}_3$ in a shell ε_2 is equal to the uniform field within the effective particle with permittivity tensor $\hat{\varepsilon}_{eff}$. For the effective homogeneous particle we can write

$$\begin{aligned}\langle\vec{E}\rangle_{\Omega_2\cup\Omega_3} &= \frac{1}{\mu(\Omega_2\cup\Omega_3)}\int_{\Omega_2\cup\Omega_3}\vec{E}(\vec{x})d\vec{x} \\ &= -\frac{1}{\mu(\Omega_2\cup\Omega_3)}\int_{\Omega_2\cup\Omega_3}\frac{\partial\phi(\vec{x})}{\partial\vec{x}}d\vec{x} = -\frac{1}{\mu(\Omega_2\cup\Omega_3)}\int_{\xi=0}\phi(\vec{x})|_{\xi=0}\,\vec{n}\,dS,\end{aligned} \tag{54}$$

where we have used the divergence theorem. Therefore, the internal average quantity is determined by the values of the electric potential $\phi(\vec{x})$ over the particle surface ($\xi = 0$), which is a continuous quantity by definition. Please note that, in this case, the region $\Omega_2\cup\Omega_3$ represents a homogeneous dielectric. Similarly, for the composite particle, we have

$$\begin{aligned}\langle\vec{E}\rangle_{\Omega_2\cup\Omega_3} &= -\frac{1}{\mu(\Omega_2\cup\Omega_3)}\left[\int_{\Omega_2}\frac{\partial\phi(\vec{x})}{\partial\vec{x}}d\vec{x} + \int_{\Omega_3}\frac{\partial\phi(\vec{x})}{\partial\vec{x}}d\vec{x}\right] \\ &= -\frac{1}{\mu(\Omega_2\cup\Omega_3)}\left[\int_{\xi=0}\phi(\vec{x})|_{\xi=0}\,\vec{n}\,dS - \int_{\xi=\xi_c}\phi(\vec{x})|_{\xi=\xi_c^+}\,\vec{n}\,dS + \int_{\xi=\xi_c}\phi(\vec{x})|_{\xi=\xi_c^-}\,\vec{n}\,dS\right].\end{aligned} \tag{55}$$

Now, the continuity of the electric potential affirms that $\phi(\vec{x})|_{\xi=\xi_c^+} = \phi(\vec{x})|_{\xi=\xi_c^-}$ and, therefore, Eqs. (54) and (55) assume the same value. Finally, the average electric field is the same in the effective homogeneous and composite particles since the external field is imposed equal in both cases. This equivalence property can be used to determine the average value of the electric field in the shell region $\langle\vec{E}_s\rangle_{\Omega_2}$. Indeed, the equivalence property can be explicitly stated as $-\vec{C}_{hom} = -c\vec{C} + (1-c)\langle\vec{E}_s\rangle_{\Omega_2}$ where in $\vec{C}_{hom}$ we consider $\hat{\varepsilon}_3 = \hat{\varepsilon}_{eff}$ and where $c = A_c/A_s$ is the volume fraction of the core in the shell. Of course, in previous expression, $-\vec{C}_{hom}$ represent the average (uniform) value of the electric field in the effective particle and $-c\vec{C} + (1-c)\langle\vec{E}_s\rangle_{\Omega_2}$ the average electric field in the composite one. Anyway, this equality can be rewritten as follows by taking into account Eqs. (46) and (50)

$$\varepsilon_1\left[\varepsilon_1\hat{I}+\hat{L}_s\left(\hat{\varepsilon}_{eff}-\varepsilon_1\hat{I}\right)\right]^{-1}\vec{E}_0=-c\varepsilon_1\varepsilon_2A_s\hat{D}^{-1}\vec{E}_0+(1-c)\langle\vec{E}_s\rangle_{\Omega_2},\tag{56}$$

where $\hat{\varepsilon}_{eff}$ is given in Eq. (52). This equation can be solved with respect to $\langle\vec{E}_s\rangle_{\Omega_2}$, by eventually obtaining

$$\langle\vec{E}_s\rangle_{\Omega_2}=-\varepsilon_1A_s\left\{\left[\hat{L}_c+\frac{A_c}{A_c-A_s}\left(\hat{L}_s-\hat{L}_c\right)\right]\left(\hat{\varepsilon}_3-\varepsilon_2\hat{I}\right)+\varepsilon_2\hat{I}\right\}\hat{D}^{-1}\vec{E}_0,\tag{57}$$

or, equivalently,

$$\langle\vec{E}_s\rangle_{\Omega_2}=-\varepsilon_1A_s\left\{\left[\hat{L}_c+\frac{c}{1-c}\left(\hat{L}_c-\hat{L}_s\right)\right]\left(\hat{\varepsilon}_3-\varepsilon_2\hat{I}\right)+\varepsilon_2\hat{I}\right\}\hat{D}^{-1}\vec{E}_0.\tag{58}$$

To conclude, this is the exact expression giving the average electric field within the shell region. It is important to remark that we obtain $\langle\vec{E}_s\rangle_{\Omega_2}=-\vec{S}$ (by comparing Eqs. (45) and (58)), i.e. the average value in the shell corresponds only to the uniform contribution in Eq. (13), if and only if $\hat{L}_c=\hat{L}_s$, a condition satisfied only for spherical or cylindrical geometries (or in the trivial case without shell, $c=0$). In fact, the non-uniform term in Eq. (13), controlled by the vector coefficient $\vec{T}$, has a zero contribution for spherical or cylindrical geometries since it corresponds to the classical dipolar behavior; on the other hand, for an arbitrary ellipsoidal geometry this dipolar property is not verified and we have $\langle\vec{E}_s\rangle_{\Omega_2}\neq-\vec{S}$, being the deviation between these quantities controlled by the difference $\hat{L}_s-\hat{L}_c$ and by the volume fraction c.

4. Generalization to constitutive equations with temporal dispersion

The results of previous Section can be generalized to consider more complex constitutive equations, notably describing linear and nonlinear temporal dispersion. As discussed in Section 2, shells and matrix are described by the complex valued permittivities $\dot{\varepsilon}_2(\omega)$ and $\dot{\varepsilon}_1(\omega)$, respectively. Because of the linearity of the system, all results of previous Section are still valid provided that each quantity is substituted by its phasor. Moreover, the core of the particles is described by the field dependent permittivity tensor given in Eq. (8) of Section 2. The consideration of this response is more complicated and the corresponding problem can be solved as follows. In spite of the nonlinear character of Eq. (8), we can affirm that the uniformity of the electric field inside the core is confirmed also in this case (Giordano & Rocchia, 2005). The equation for obtaining this uniform internal field, see Eq. (46), remains unaltered, even though it assumes an implicit form. Indeed, by substituting the constitutive equation $\dot{\vec{D}}_c(\vec{x},\omega)=\dot{\hat{\varepsilon}}_{3,tot}(\omega)\dot{\vec{E}}_c(\vec{x},\omega)$ in the relation giving the internal electric field (inside the core, see Eq. (46)), i.e.

$$\dot{\hat{D}}\dot{\vec{E}}_c=-\dot{\varepsilon}_1\dot{\varepsilon}_2A_s\dot{\vec{E}}_0,\tag{59}$$

we obtain

$$\dot{\hat{\alpha}}\dot{\vec{E}}_c+\frac{1}{2}\chi_1\dot{\hat{\beta}}\left(\dot{\vec{E}}_c\cdot\dot{\vec{E}}_c^*\right)\dot{\vec{E}}_c+\frac{1}{4}\chi_2\dot{\hat{\beta}}\left(\dot{\vec{E}}_c\cdot\dot{\vec{E}}_c\right)\dot{\vec{E}}_c^*=\dot{\vec{E}}_0,\tag{60}$$

where

$$\begin{aligned}\dot{\hat{\alpha}}=&-\frac{c}{\dot{\varepsilon}_1\dot{\varepsilon}_2}(\dot{\varepsilon}_2-\dot{\varepsilon}_1)\hat{L}_s\left(\hat{L}_s-\hat{I}\right)\left(\dot{\varepsilon}_3-\dot{\varepsilon}_2\hat{I}\right)\\&+\frac{1}{\dot{\varepsilon}_1\dot{\varepsilon}_2}\left[\dot{\varepsilon}_1\hat{I}+\hat{L}_s(\dot{\varepsilon}_2-\dot{\varepsilon}_1)\right]\left[\dot{\varepsilon}_2\hat{I}+\hat{L}_c\left(\dot{\varepsilon}_3-\dot{\varepsilon}_2\hat{I}\right)\right],\end{aligned}\tag{61}$$

$$\dot{\hat{\beta}}=-\frac{c}{\dot{\varepsilon}_1\dot{\varepsilon}_2}(\dot{\varepsilon}_2-\dot{\varepsilon}_1)\hat{L}_s\left(\hat{L}_s-\hat{I}\right)+\frac{1}{\dot{\varepsilon}_1\dot{\varepsilon}_2}\left[\dot{\varepsilon}_1\hat{I}+\hat{L}_s(\dot{\varepsilon}_2-\dot{\varepsilon}_1)\right]\hat{L}_c,\tag{62}$$

are diagonal operators with components $\dot{\alpha}_k$ and $\dot{\beta}_k$, respectively. Here, as before, $c=A_c/A_s$ represents the volume fraction of the core within the shell. If a solution of Eq. (60) exists, due to self-consistency, all the boundary conditions are fulfilled and the problem is completely analogous to its linear counterpart, treated in the previous Section. In its explicit form, Eq. (60) can be rewritten as

$$\dot{\alpha}_k\dot{E}_{ck}+\frac{1}{2}\chi_1\dot{\beta}_k\dot{E}_{ck}\sum_i\dot{E}_{ci}\dot{E}_{ci}^*+\frac{1}{4}\chi_2\dot{\beta}_k\dot{E}_{ck}^*\sum_i\dot{E}_{ci}^2=\dot{E}_{0k}.\tag{63}$$

By considering a possible solution of the form $\dot{E}_{ck}=\dot{a}_k\dot{E}_{0k}+\dot{b}_k\dot{E}_{0k}^3$, it is not difficult to obtain the expression of $\dot{E}_{ck}$ in terms of $\dot{E}_{0k}$, expanded up to the third order

$$\dot{E}_{ck}=\frac{1}{\dot{\alpha}_k}\dot{E}_{0k}-\frac{1}{2}\chi_1\frac{\dot{\beta}_k}{\dot{\alpha}_k^2}\dot{E}_{0k}\sum_i\frac{\dot{E}_{0i}\dot{E}_{0i}^*}{\dot{\alpha}_i\dot{\alpha}_i^*}-\frac{1}{4}\chi_2\frac{\dot{\beta}_k}{\dot{\alpha}_k\dot{\alpha}_k^*}\dot{E}_{0k}^*\sum_i\frac{\dot{E}_{0i}^2}{\dot{\alpha}_i^2}.\tag{64}$$

This result represents the electric field phasor inside the nonlinear core of a composite particle embedded in a given matrix. To sum up we remember that the three phases core, shell and matrix are described by the complex frequency dependent permittivities $\dot{\varepsilon}_3, \dot{\varepsilon}_2$ and $\dot{\varepsilon}_1$, respectively; moreover, the core exhibits a nonlinear behavior modulated by the complex nonlinear susceptibilities $\dot{\chi}_1(\omega) = \dot{\chi}(0,\omega)$ and $\dot{\chi}_2(\omega) = \dot{\chi}(2\omega,\omega)$. The final result stated in Eq. (64) is completly controlled by the quantities $\dot{\alpha}_k$ and $\dot{\beta}_k$, defined in Eqs. (61) and (62).

Of course, the presence of the above discussed nonlinear behavior for the core alters the average value of the electric field within the shell region. However, by considering Eqs. (57) and (59) we can rewrite the average value of the electric field over the shell region in terms of the value of the electric field within the core

$$\begin{aligned}
\langle \dot{\vec{E}}_s \rangle_{\Omega_2} &= \frac{1}{\dot{\varepsilon}_2}\left\{\left[\hat{L}_c + \frac{A_c}{A_c - A_s}\left(\hat{L}_s - \hat{L}_c\right)\right]\left(\hat{\dot{\varepsilon}}_{3,tot} - \dot{\varepsilon}_2\hat{I}\right) + \dot{\varepsilon}_2\hat{I}\right\}\dot{\vec{E}}_c \\
&= \frac{1}{\dot{\varepsilon}_2}\left[\hat{L}_c + \frac{A_c}{A_c - A_s}\left(\hat{L}_s - \hat{L}_c\right)\right]\left[\hat{\dot{\varepsilon}}_3\dot{\vec{E}}_c + \frac{1}{2}\dot{\chi}_1\left(\dot{\vec{E}}_c \cdot \dot{\vec{E}}_c^*\right)\dot{\vec{E}}_c + \frac{1}{4}\dot{\chi}_2\left(\dot{\vec{E}}_c \cdot \dot{\vec{E}}_c\right)\dot{\vec{E}}_c^*\right] \\
&\quad + \left\{\hat{I} - \left[\hat{L}_c + \frac{A_c}{A_c - A_s}\left(\hat{L}_s - \hat{L}_c\right)\right]\right\}\dot{\vec{E}}_c.
\end{aligned} \tag{65}$$

Of course, in Eq. (57) we have introduced the complete expression for $\hat{\dot{\varepsilon}}_{3,tot}$ given in Eq. (8) in place of the standard tensor $\hat{\dot{\varepsilon}}_3$. Now, we can rewrite Eq. (65) component-by-component and we may exploit the result $\frac{1}{2}\dot{\chi}_1\dot{E}_{ck}\sum_i \dot{E}_{ci}\dot{E}_{ci}^* + \frac{1}{4}\dot{\chi}_2\dot{E}_{ck}^*\sum_i \dot{E}_{ci}^2 = (\dot{E}_{0k} - \dot{\alpha}_k\dot{E}_{ck})/\dot{\beta}_k$, coming directly from Eq. (63). The result of this procedure can be eventually obtained as

$$\begin{aligned}
\langle \dot{E}_{sk} \rangle_{\Omega_2} &= \frac{1}{\dot{\varepsilon}_2}\left[L_{ck} + \frac{A_c}{A_c - A_s}(L_{sk} - L_{ck})\right]\left[\dot{\varepsilon}_3\dot{E}_{ck} + \frac{\dot{E}_{0k} - \dot{\alpha}_k\dot{E}_{ck}}{\dot{\beta}_k}\right] \\
&\quad + \left\{1 - \left[L_{ck} + \frac{A_c}{A_c - A_s}(L_{sk} - L_{ck})\right]\right\}\dot{E}_{ck} \\
&= \dot{t}_k\dot{E}_{ck} + \frac{\dot{s}_k}{\dot{\varepsilon}_2\dot{\beta}_k}\dot{E}_{0k}
\end{aligned} \tag{66}$$

where

$$\dot{s}_k = L_{ck} + \frac{A_c}{A_c - A_s}(L_{sk} - L_{ck}) = L_{ck} + \frac{c}{1-c}(L_{ck} - L_{sk}) \tag{67}$$

$$\dot{t}_k = 1 - \dot{s}_k + \frac{\dot{\varepsilon}_3}{\dot{\varepsilon}_2}\dot{s}_k - \frac{\dot{s}_k\dot{\alpha}_k}{\dot{\varepsilon}_2\dot{\beta}_k} \tag{68}$$

This completes the determination of the electric field in the nonlinear core and in the shell of the composite particle.

5. Averaging procedure over the orientations

In previous Section we have obtained the results for $\dot{E}_{ck}$ and $\langle \dot{E}_{sk} \rangle_{\Omega_2}$, representing the electric fields in the core and in the shell (averaged), respectively, for a composite particle having the principal axes aligned with the coordinate system. These results give the final quantities in terms of the remotely applied electric field, arbitrarily oriented in the space. Now, we maintain fixed the vector corresponding to the applied field and we consider the particle uniformly randomly oriented in the space (see Fig. 3 for details). So doing, we are interested in determining the average value of the quantities $\dot{E}_{ck}$ and $\langle \dot{E}_{sk} \rangle_{\Omega_2}$ over the Euler angles ϑ, ψ and φ, controlling the orientation of the particle in the space. In the following, these averaged fields will be referred to as $\langle \dot{E}_{ck} \rangle_{\vartheta,\psi,\varphi}$ and $\langle\langle \dot{E}_{sk} \rangle_{\Omega_2}\rangle_{\vartheta,\psi,\varphi}$. Of course, we have obtained in Eqs. (64) and (66) a non isotropic relationship giving $\dot{E}_{ck}$ and $\langle \dot{E}_{sk} \rangle_{\Omega_2}$ as function of $\dot{E}_{0k}$, because of the ellipsoidal (geometrically non isotropic) shape of the particle. On the contrary, after having performed the averaging we will obtain an isotropic relation between $\langle \dot{E}_{ck} \rangle_{\vartheta,\psi,\varphi}$ or $\langle\langle \dot{E}_{sk} \rangle_{\Omega_2}\rangle_{\vartheta,\psi,\varphi}$ and the applied field $\dot{E}_{0k}$ since the angles averaging smears out the shape anisotropy. The final isotropic relation will therefore assume a form similar to that of Eq. (5).

To begin the calculation, we note that in Eq. (66) for $\langle \dot{E}_{sk} \rangle_{\Omega_2}$ there is a first term $\dot{E}_{ck}\dot{t}_k$. Therefore, we firstly determine the average value of this quantity, observing that, for obtaining the average value of $\dot{E}_{ck}$, it is sufficient to substitute $\dot{t}_k = 1$ in the final result. Moreover, we will analyse the second term in Eq. (66) to complete the calculation. Hence, we consider the following vector components

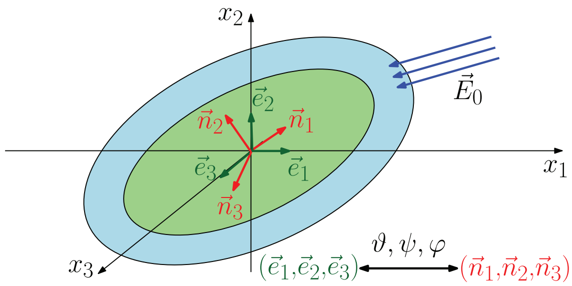

Fig. 3. Rotation of the confocal core–shell structure, representing the composite particle.

$$\dot{v}_k = \dot{E}_{ck}\dot{t}_k = \frac{\dot{t}_k}{\dot{\alpha}_k}\dot{E}_{0k} - \frac{1}{2}\dot{\chi}_1\frac{\dot{\beta}_k\dot{t}_k}{\dot{\alpha}_k^2}\dot{E}_{0k}\sum_i\frac{\dot{E}_{0i}\dot{E}_{0i}^*}{\dot{\alpha}_i\dot{\alpha}_i^*} - \frac{1}{4}\dot{\chi}_2\frac{\dot{\beta}_k\dot{t}_k}{\dot{\alpha}_k\dot{\alpha}_k^*}\dot{E}_{0k}^*\sum_i\frac{\dot{E}_{0i}^2}{\dot{\alpha}_i^2}, \tag{69}$$

and we try to calculate the average value over the orientation. To do this, we define the principal directions of the rotated particle as $\vec{n}_1$, $\vec{n}_2$ and $\vec{n}_3$, useful to write the average value in the following form

$$\langle\dot{\vec{v}}\rangle_{\vartheta,\psi,\varphi} = \left\langle\sum_k \dot{v}_k\vec{n}_k\right\rangle_{\vartheta,\psi,\varphi} = \left\langle\sum_k\left[\frac{\dot{t}_k}{\dot{\alpha}_k}\dot{\vec{E}}_0\cdot\vec{n}_k - \frac{1}{2}\dot{\chi}_1\frac{\dot{\beta}_k\dot{t}_k}{\dot{\alpha}_k^2}\dot{\vec{E}}_0\cdot\vec{n}_k\sum_i\frac{\left(\dot{\vec{E}}_0\cdot\vec{n}_i\right)\left(\dot{\vec{E}}_0^*\cdot\vec{n}_i\right)}{\dot{\alpha}_i\dot{\alpha}_i^*} - \frac{1}{4}\dot{\chi}_2\frac{\dot{\beta}_k\dot{t}_k}{\dot{\alpha}_k\dot{\alpha}_k^*}\dot{\vec{E}}_0^*\cdot\vec{n}_k\sum_i\frac{\left(\dot{\vec{E}}_0\cdot\vec{n}_i\right)^2}{\dot{\alpha}_i^2}\right]\vec{n}_k\right\rangle_{\vartheta,\psi,\varphi}, \tag{70}$$

where we exploited the standard properties $\dot{\vec{v}} = \sum_k \dot{v}_k\vec{n}_k$ and $\dot{E}_{0k} = \dot{\vec{E}}_0\cdot\vec{n}_k$. By further expanding Eq. (70) (or, more precisely, its s-th component), we easily obtain

$$\begin{aligned}\langle\dot{v}_s\rangle_{\vartheta,\psi,\varphi} = &\sum_{kj}\frac{\dot{t}_k}{\dot{\alpha}_k}\dot{E}_{0j}\langle n_{kj}n_{ks}\rangle_{\vartheta,\psi,\varphi} - \frac{1}{2}\dot{\chi}_1\sum_{iklqp}\frac{\dot{\beta}_k\dot{t}_k}{\dot{\alpha}_k^2}\frac{\dot{E}_{0l}\dot{E}_{0q}\dot{E}_{0p}^*}{\dot{\alpha}_i\dot{\alpha}_i^*}\langle n_{kl}n_{iq}n_{ip}n_{ks}\rangle_{\vartheta,\psi,\varphi}\\ &-\frac{1}{4}\dot{\chi}_2\sum_{iklqp}\frac{\dot{\beta}_k\dot{t}_k}{\dot{\alpha}_k\dot{\alpha}_k^*}\frac{\dot{E}_{0l}^*\dot{E}_{0q}\dot{E}_{0p}}{\dot{\alpha}_i^2}\langle n_{kl}n_{iq}n_{ip}n_{ks}\rangle_{\vartheta,\psi,\varphi},\end{aligned} \tag{71}$$

where n_{kj} represents the jth component of the unit vector $\vec{n}_k$. Now, the problem is solved if we are able to calculate the average value of the combinations $n_{kj}n_{ks}$ and $n_{kl}n_{iq}n_{ip}n_{ks}$ over the random orientations of the orthogonal unit vectors $\vec{n}_1$, $\vec{n}_2$ and $\vec{n}_3$. Performing the integration over the unit sphere, by means of standard spherical coordinates, we obtain, after some long but straightforward computations, the results

$$\langle n_{kj}n_{ks}\rangle_{\vartheta,\psi,\varphi} = \frac{1}{3}\delta_{js}, \tag{72}$$

$$\langle n_{kl}n_{iq}n_{ip}n_{ks}\rangle_{\vartheta,\psi,\varphi} = \frac{1}{15}\left(2\delta_{ls}\delta_{qp} - \frac{1}{2}\delta_{ql}\delta_{ps} - \frac{1}{2}\delta_{qs}\delta_{pl}\right) - \frac{1}{15}\delta_{ik}\left(\delta_{ls}\delta_{qp} - \frac{3}{2}\delta_{ql}\delta_{ps} - \frac{3}{2}\delta_{qs}\delta_{pl}\right). \tag{73}$$

We remark that these expressions are in perfect agreement with previous literature (Giordano & Rocchia, 2005). It is also interesting to note that such a rotational averaging has been thoroughly examined to calculate the macroscopic response of isotropic and anisotropic samples from microscopic parameters, an idea perfectly coherent with the present investigation (Andrews, 2004). Anyway, by substituting Eqs. (72) and (73) in Eq. (71), we obtain

$$\begin{aligned}\langle\dot{v}_s\rangle_{\vartheta,\psi,\varphi} = &\frac{1}{3}\sum_{kj}\frac{\dot{t}_k}{\dot{\alpha}_k}\dot{E}_{0j}\delta_{js}\\ &-\frac{1}{2}\dot{\chi}_1\sum_{iklqp}\frac{\dot{\beta}_k\dot{t}_k}{\dot{\alpha}_k^2}\frac{\dot{E}_{0l}\dot{E}_{0q}\dot{E}_{0p}^*}{\dot{\alpha}_i\dot{\alpha}_i^*}\frac{1}{15}\left(2\delta_{ls}\delta_{qp} - \frac{1}{2}\delta_{ql}\delta_{ps} - \frac{1}{2}\delta_{qs}\delta_{pl}\right)\\ &+\frac{1}{2}\dot{\chi}_1\sum_{iklqp}\frac{\dot{\beta}_k\dot{t}_k}{\dot{\alpha}_k^2}\frac{\dot{E}_{0l}\dot{E}_{0q}\dot{E}_{0p}^*}{\dot{\alpha}_i\dot{\alpha}_i^*}\frac{1}{15}\delta_{ik}\left(\delta_{ls}\delta_{qp} - \frac{3}{2}\delta_{ql}\delta_{ps} - \frac{3}{2}\delta_{qs}\delta_{pl}\right)\\ &-\frac{1}{4}\dot{\chi}_2\sum_{iklqp}\frac{\dot{\beta}_k\dot{t}_k}{\dot{\alpha}_k\dot{\alpha}_k^*}\frac{\dot{E}_{0l}^*\dot{E}_{0q}\dot{E}_{0p}}{\dot{\alpha}_i^2}\frac{1}{15}\left(2\delta_{ls}\delta_{qp} - \frac{1}{2}\delta_{ql}\delta_{ps} - \frac{1}{2}\delta_{qs}\delta_{pl}\right)\\ &+\frac{1}{4}\dot{\chi}_2\sum_{iklqp}\frac{\dot{\beta}_k\dot{t}_k}{\dot{\alpha}_k\dot{\alpha}_k^*}\frac{\dot{E}_{0l}^*\dot{E}_{0q}\dot{E}_{0p}}{\dot{\alpha}_i^2}\frac{1}{15}\delta_{ik}\left(\delta_{ls}\delta_{qp} - \frac{3}{2}\delta_{ql}\delta_{ps} - \frac{3}{2}\delta_{qs}\delta_{pl}\right),\end{aligned} \tag{74}$$

and, by saturating all the sums over repeated indices, we finally obtain

$$\begin{aligned}\langle \dot{v}_s\rangle_{\vartheta,\psi,\varphi} &= \mathcal{M}_t\dot{E}_{0s} \\ &\quad -\frac{1}{2}\dot{\chi}_1\dot{E}_{0s}\sum_q \dot{E}_{0q}\dot{E}^*_{0q}\left(\frac{9}{10}\mathcal{X}_t+\frac{1}{10}\mathcal{Z}_t\right)-\frac{3}{20}\dot{\chi}_1\dot{E}^*_{0s}\sum_q \dot{E}_{0q}\dot{E}_{0q}(\mathcal{Z}_t-\mathcal{X}_t) \\ &\quad -\frac{3}{20}\dot{\chi}_2\dot{E}_{0s}\sum_q \dot{E}_{0q}\dot{E}^*_{0q}(\mathcal{Z}_t-\mathcal{Y}_t)-\frac{1}{4}\dot{\chi}_2\dot{E}^*_{0s}\sum_q \dot{E}_{0q}\dot{E}_{0q}\left(\frac{6}{5}\mathcal{Y}_t-\frac{1}{5}\mathcal{Z}_t\right) \\ &= \mathcal{M}_t\dot{E}_{0s}-\mathcal{A}_t\dot{E}_{0s}\sum_q \dot{E}_{0q}\dot{E}^*_{0q}-\mathcal{B}_t\dot{E}^*_{0s}\sum_q \dot{E}_{0q}\dot{E}_{0q},\end{aligned} \tag{75}$$

where we defined

$$\mathcal{M}_t = \frac{1}{3}\sum_k \frac{\dot{t}_k}{\dot{\alpha}_k}, \tag{76}$$

$$\mathcal{X}_t = \left(\frac{1}{3}\sum_k \frac{\dot{\beta}_k\dot{t}_k}{\dot{\alpha}_k^2}\right)\left(\frac{1}{3}\sum_i \frac{1}{\dot{\alpha}_i\dot{\alpha}_i^*}\right), \tag{77}$$

$$\mathcal{Y}_t = \left(\frac{1}{3}\sum_k \frac{\dot{\beta}_k\dot{t}_k}{\dot{\alpha}_k\dot{\alpha}_k^*}\right)\left(\frac{1}{3}\sum_i \frac{1}{\dot{\alpha}_i^2}\right), \tag{78}$$

$$\mathcal{Z}_t = \frac{1}{3}\sum_k \frac{\dot{\beta}_k\dot{t}_k}{\dot{\alpha}_k^3\dot{\alpha}_k^*}, \tag{79}$$

$$\mathcal{A}_t = \frac{1}{2}\dot{\chi}_1\left(\frac{9}{10}\mathcal{X}_t+\frac{1}{10}\mathcal{Z}_t\right)-\frac{3}{20}\dot{\chi}_2(\mathcal{Y}_t-\mathcal{Z}_t), \tag{80}$$

$$\mathcal{B}_t = \frac{1}{4}\dot{\chi}_2\left(\frac{6}{5}\mathcal{Y}_t-\frac{1}{5}\mathcal{Z}_t\right)-\frac{3}{20}\dot{\chi}_1(\mathcal{X}_t-\mathcal{Z}_t). \tag{81}$$

In order to complete the determination of the average value of $\langle \dot{E}_{sk}\rangle_{\Omega_2}$ we have to consider the second term in Eq. (66), which corresponds to $\dot{s}_k/(\dot{\varepsilon}_2\dot{\beta}_k)\dot{E}_{0k}$. Its average value (we consider the s-th component) over the orientations can be simply determined as follows

$$\left\langle \sum_k \frac{\dot{s}_k}{\dot{\varepsilon}_2\dot{\beta}_k}\left(\vec{\dot{E}}_0\cdot\vec{n}_k\right)n_{ks}\right\rangle_{\vartheta,\psi,\varphi} = \sum_{k,i}\frac{\dot{s}_k}{\dot{\varepsilon}_2\dot{\beta}_k}\dot{E}_{0i}\langle n_{ki}n_{ks}\rangle_{\vartheta,\psi,\varphi} = \frac{1}{3}\sum_k \frac{\dot{s}_k}{\dot{\varepsilon}_2\dot{\beta}_k}\dot{E}_{0s}. \tag{82}$$

By adding Eqs. (75) and (82) we obtain the first important result giving the average value of the electric field within the shell region

$$\left\langle \langle \dot{E}_{sk}\rangle_{\Omega_2}\right\rangle_{\vartheta,\psi,\varphi} = \Psi\dot{E}_{0s}-\mathcal{A}_t\dot{E}_{0k}\sum_q \dot{E}_{0q}\dot{E}^*_{0q}-\mathcal{B}_t\dot{E}^*_{0k}\sum_q \dot{E}_{0q}\dot{E}_{0q}, \tag{83}$$

where we introduced the parameter Ψ as follows

$$\Psi = \frac{1}{3\dot{\varepsilon}_2}\sum_k \frac{\dot{s}_k}{\dot{\beta}_k}+\frac{1}{3}\sum_k \frac{\dot{t}_k}{\dot{\alpha}_k}. \tag{84}$$

To conclude, we observe that by letting $\dot{t}_k = 1$ in Eq. (75), we directly obtain the angular averaged value of $\dot{E}_{ck}$ inside the particle core

$$\langle \dot{E}_{ck}\rangle_{\vartheta,\psi,\varphi} = \mathcal{M}\dot{E}_{0s}-\mathcal{A}\dot{E}_{0k}\sum_q \dot{E}_{0q}\dot{E}^*_{0q}-\mathcal{B}\dot{E}^*_{0k}\sum_q \dot{E}_{0q}\dot{E}_{0q}, \tag{85}$$

where the following parameters have been used

$$\mathcal{M} = \frac{1}{3}\sum_k \frac{1}{\dot{\alpha}_k}, \tag{86}$$

$$\mathcal{X} = \left(\frac{1}{3}\sum_k \frac{\dot{\beta}_k}{\dot{\alpha}_k^2}\right)\left(\frac{1}{3}\sum_i \frac{1}{\dot{\alpha}_i\dot{\alpha}_i^*}\right), \tag{87}$$

$$\mathcal{Y} = \left(\frac{1}{3}\sum_k \frac{\dot{\beta}_k}{\dot{\alpha}_k\dot{\alpha}_k^*}\right)\left(\frac{1}{3}\sum_i \frac{1}{\dot{\alpha}_i^2}\right), \tag{88}$$

$$\mathcal{Z} = \frac{1}{3}\sum_k \frac{\dot{\beta}_k}{\dot{\alpha}_k^3\dot{\alpha}_k^*}, \tag{89}$$

$$\mathcal{A} = \frac{1}{2}\dot{\chi}_1\left(\frac{9}{10}\mathcal{X} + \frac{1}{10}\mathcal{Z}\right) - \frac{3}{20}\dot{\chi}_2(\mathcal{Y} - \mathcal{Z}), \tag{90}$$

$$\mathcal{B} = \frac{1}{4}\dot{\chi}_2\left(\frac{6}{5}\mathcal{Y} - \frac{1}{5}\mathcal{Z}\right) - \frac{3}{20}\dot{\chi}_1(\mathcal{X} - \mathcal{Z}), \tag{91}$$

and they can be simply obtained by letting $\dot{t}_k = 1$ in Eqs. (76)–(81). We finally remark that Eqs. (83) and (85) represent isotropic relationships between the remotely applied field and the internal average ones. Indeed, they exhibit the same form of the isotropic constitutive equation stated in Eq. (5).

6. Effective medium theory for a population of randomly oriented particles

We consider in this Section a population of composite particles randomly oriented and dispersed in the matrix. As before, we suppose to deal with nonlinear cores and linear materials for shells and matrix. The structure is represented in Fig. 1, where one can find the definition of the regions Ω_m (matrix), Ω_s (ensemble of shells) and Ω_c (ensemble of cores). Moreover, we consider the whole composite structure contained in the region Ω, representing the body we are going to homogenize. Because of the random orientations of the particle, we expect to find an overall isotropic response for the entire composite material. It means that it will be described by an isotropic constitutive equation, having the form given in Eq. (5), where we will introduce an effective complex permittivity $\dot{\varepsilon}_{eff}(\omega)$ and by two nonlinear susceptibilities $\dot{\chi}_{1,eff}(\omega)$ and $\dot{\chi}_{2,eff}(\omega)$. In order to develop the effective medium theory we need to determine the average value of the displacement vector and of the electric field over the whole region Ω. We begin by evaluating the average value of the vector $\dot{\vec{D}}$, as follows

$$\begin{aligned}
\langle\dot{\vec{D}}\rangle &= \frac{1}{\mu(\Omega)}\int_{\Omega}\dot{\vec{D}}dv = \frac{1}{\mu(\Omega)}\int_{\Omega_m}\dot{\vec{D}}dv + \frac{1}{\mu(\Omega)}\int_{\Omega_s}\dot{\vec{D}}dv + \frac{1}{\mu(\Omega)}\int_{\Omega_c}\dot{\vec{D}}dv \\
&= \frac{1}{\mu(\Omega)}\int_{\Omega_m}\dot{\vec{D}}dv + \frac{1}{\mu(\Omega)}\int_{\Omega_s}\dot{\vec{D}}dv + \frac{1}{\mu(\Omega)}\int_{\Omega_c}\dot{\vec{D}}dv \\
&\quad + \frac{\dot{\varepsilon}_1}{\mu(\Omega)}\int_{\Omega_s}\dot{\vec{E}}dv - \frac{\dot{\varepsilon}_1}{\mu(\Omega)}\int_{\Omega_s}\dot{\vec{E}}dv + \frac{\dot{\varepsilon}_1}{\mu(\Omega)}\int_{\Omega_c}\dot{\vec{E}}dv - \frac{\dot{\varepsilon}_1}{\mu(\Omega)}\int_{\Omega_c}\dot{\vec{E}}dv \\
&= \frac{1}{\mu(\Omega)}\dot{\varepsilon}_1\int_{\Omega}\dot{\vec{E}}dv + \frac{1}{\mu(\Omega)}(\dot{\varepsilon}_2 - \dot{\varepsilon}_1)\int_{\Omega_s}\dot{\vec{E}}dv + \frac{1}{\mu(\Omega)}\int_{\Omega_c}\left(\dot{\vec{D}} - \dot{\varepsilon}_1\dot{\vec{E}}\right)dv \\
&= \dot{\varepsilon}_1\langle\dot{\vec{E}}\rangle + \phi(1-c)(\dot{\varepsilon}_2 - \dot{\varepsilon}_1)\langle\dot{\vec{E}}_s\rangle_{\Omega_s} + \phi c\left\langle\dot{\vec{D}}_c - \dot{\varepsilon}_1\dot{\vec{E}}_c\right\rangle_{\Omega_c} \\
&\cong \dot{\varepsilon}_1\langle\dot{\vec{E}}\rangle + \phi(1-c)(\dot{\varepsilon}_2 - \dot{\varepsilon}_1)\left\langle\left\langle\dot{\vec{E}}_s\right\rangle_{\Omega_2}\right\rangle_{\vartheta,\psi,\varphi} + \phi c\left\langle\dot{\vec{D}}_c - \dot{\varepsilon}_1\dot{\vec{E}}_c\right\rangle_{\vartheta,\psi,\varphi},
\end{aligned} \tag{92}$$

where we have considered the volume fraction c of the core within each composite particle and the volume fraction ϕ of the particles in the entire volume (see definitions in Fig. 1). They represent the stoichiometric parameters of the heterogeneous structure. In previous expression, the symbol $\mu(\Omega)$ represents the measure of the region Ω. The second to last expression is an exact result giving the average value of $\dot{\vec{D}}$ in terms of $\langle\dot{\vec{E}}\rangle$, $\langle\dot{\vec{E}}_s\rangle_{\Omega_s}$ and $\langle\dot{\vec{D}}_c - \dot{\varepsilon}_1\dot{\vec{E}}_c\rangle_{\Omega_c}$. From now on, we introduce the hypothesis to work with a dilute dispersion of particle, i.e. $\phi \ll 1$. Conversely, the theory is valid for any value of the volume fraction c, describing the composition of the particles. So doing, each particle can be considered as isolated in the space and subjected to a remotely applied field, as discussed in previous Sections. Hence, the value $\langle\dot{\vec{E}}_s\rangle_{\Omega_s}$ can be approximated with $\langle\langle\dot{\vec{E}}_s\rangle_{\Omega_2}\rangle_{\vartheta,\psi,\varphi}$, calculated in the previous Section for an isolated particle, see Eq. (83). Similarly, the last term $\langle\dot{\vec{D}}_c - \dot{\varepsilon}_1\dot{\vec{E}}_c\rangle_{\Omega_c}$ can be approximately evaluated by considering a single particle in the matrix. This approximation will be referred to as $\langle\dot{\vec{D}}_c - \dot{\varepsilon}_1\dot{\vec{E}}_c\rangle_{\vartheta,\psi,\varphi}$ and this quantity must be evaluated in the following. Anyway, these approximations lead to the final result given in Eq. (92).

We can follow a similar procedure for the average value of the electric field. We obtain the following result

$$\begin{aligned}
\langle\dot{\vec{E}}\rangle &= (1-\phi)\langle\dot{\vec{E}}_m\rangle_{\Omega_m} + \phi(1-c)\langle\dot{\vec{E}}_s\rangle_{\Omega_s} + \phi c\langle\dot{\vec{E}}_c\rangle_{\Omega_c} \\
&\cong (1-\phi)\dot{\vec{E}}_0 + \phi(1-c)\langle\langle\dot{\vec{E}}_s\rangle_{\Omega_2}\rangle_{\vartheta,\psi,\varphi} + \phi c\langle\dot{\vec{E}}_c\rangle_{\vartheta,\psi,\varphi}.
\end{aligned} \tag{93}$$

While the first expression is exact and simply corresponds to the average value definition, the second one contains the approximations imposed by the hypothesis of low concentration of particles. Importantly, the terms $\langle\langle\dot{\vec{E}}_s\rangle_{\Omega_2}\rangle_{\vartheta,\psi,\varphi}$ and $\langle\dot{\vec{E}}_c\rangle_{\vartheta,\psi,\varphi}$ are available in previous Section, see Eqs. (83) and (85).

In order to obtain an explicit form of these average balance equations, we need to evaluate the term $\langle \dot{\vec{D}}_c - \dot{\varepsilon}_1 \dot{\vec{E}}_c \rangle_{\vartheta,\psi,\varphi}$, which is not available from previous calculations. We firstly observe that

$$\begin{aligned} \dot{D}_{ck} - \dot{\varepsilon}_1 \dot{E}_{ck} &= \dot{\varepsilon}_3 \dot{E}_{ck} + \frac{1}{2}\dot{\chi}_1 \dot{E}_{ck} \sum_i \dot{E}_{ci} \dot{E}_{ci}^* + \frac{1}{4}\dot{\chi}_2 \dot{E}_{ck}^* \sum_i \dot{E}_{ci}^2 - \dot{\varepsilon}_1 \dot{E}_{ck} \\ &= \dot{\varepsilon}_3 \dot{E}_{ck} + \frac{\dot{E}_{0k} - \dot{\alpha}_k \dot{E}_{ck}}{\dot{\beta}_k} - \dot{\varepsilon}_1 \dot{E}_{ck} \\ &= \frac{1}{\dot{\beta}_k} \dot{E}_{0k} + \left(\dot{\varepsilon}_3 - \dot{\varepsilon}_1 - \frac{\dot{\alpha}_k}{\dot{\beta}_k}\right) \dot{E}_{ck} = \frac{1}{\dot{\beta}_k} \dot{E}_{0k} + \dot{r}_k \dot{E}_{ck}, \end{aligned} \tag{94}$$

where we exploited the result $\frac{1}{2}\dot{\chi}_1 \dot{E}_{ck} \sum_i \dot{E}_{ci}\dot{E}_{ci}^* + \frac{1}{4}\dot{\chi}_2 \dot{E}_{ck}^* \sum_i \dot{E}_{ci}^2 = (\dot{E}_{0k} - \dot{\alpha}_k \dot{E}_{ck})/\dot{\beta}_k$, coming directly from Eq. (63), and we defined

$$\dot{r}_k = \dot{\varepsilon}_3 - \dot{\varepsilon}_1 - \frac{\dot{\alpha}_k}{\dot{\beta}_k}. \tag{95}$$

Summing up, we can apply the above discussed averaging procedure over the orientations and we eventually obtain

$$\langle \dot{D}_{ck} - \dot{\varepsilon}_1 \dot{E}_{ck} \rangle_{\vartheta,\psi,\varphi} = \mathcal{M}(\dot{\varepsilon}_3 - \dot{\varepsilon}_1)\dot{E}_{0k} - \mathcal{A}_r \dot{E}_{0k} \sum_q \dot{E}_{0q}\dot{E}_{0q}^* - \mathcal{B}_r \dot{E}_{0k}^* \sum_q \dot{E}_{0q}\dot{E}_{0q}, \tag{96}$$

where $\mathcal{M}$ is defined in Eq. (86) and the other parameters follow

$$\mathcal{X}_r = \left(\frac{1}{3}\sum_k \frac{\dot{\beta}_k \dot{r}_k}{\dot{\alpha}_k^2}\right)\left(\frac{1}{3}\sum_i \frac{1}{\dot{\alpha}_i \dot{\alpha}_i^*}\right), \tag{97}$$

$$\mathcal{Y}_r = \left(\frac{1}{3}\sum_k \frac{\dot{\beta}_k \dot{r}_k}{\dot{\alpha}_k \dot{\alpha}_k^*}\right)\left(\frac{1}{3}\sum_i \frac{1}{\dot{\alpha}_i^2}\right), \tag{98}$$

$$\mathcal{Z}_r = \frac{1}{3}\sum_k \frac{\dot{\beta}_k \dot{r}_k}{\dot{\alpha}_k^3 \dot{\alpha}_k^*}, \tag{99}$$

$$\mathcal{A}_r = \frac{1}{2}\dot{\chi}_1\left(\frac{9}{10}\mathcal{X}_r + \frac{1}{10}\mathcal{Z}_r\right) - \frac{3}{20}\dot{\chi}_2(\mathcal{Y}_r - \mathcal{Z}_r), \tag{100}$$

$$\mathcal{B}_r = \frac{1}{4}\dot{\chi}_2\left(\frac{6}{5}\mathcal{Y}_r - \frac{1}{5}\mathcal{Z}_r\right) - \frac{3}{20}\dot{\chi}_1(\mathcal{X}_r - \mathcal{Z}_r). \tag{101}$$

They can be simply obtained by substituting $\dot{t}_k$ with $\dot{r}_k$ in Eqs. (77)–(81). Now, the first balance equation for the average value of $\dot{\vec{D}}$ can be rewritten in components as follows

$$\begin{aligned} \langle \dot{D}_k \rangle &= \dot{\varepsilon}_1 \langle \dot{E}_k \rangle + \left[\phi(1-c)\Psi(\dot{\varepsilon}_2 - \dot{\varepsilon}_1) + \phi c \mathcal{M}(\dot{\varepsilon}_3 - \dot{\varepsilon}_1)\right]\dot{E}_{0k} \\ &\quad - \left[\phi(1-c)(\dot{\varepsilon}_2 - \dot{\varepsilon}_1)\mathcal{A}_t + \phi c \mathcal{A}_r\right]\dot{E}_{0k}\sum_q \dot{E}_{0q}\dot{E}_{0q}^* \\ &\quad - \left[\phi(1-c)(\dot{\varepsilon}_2 - \dot{\varepsilon}_1)\mathcal{B}_t + \phi c \mathcal{B}_r\right]\dot{E}_{0k}^*\sum_q \dot{E}_{0q}\dot{E}_{0q} \\ &= \dot{\varepsilon}_1 \langle \dot{E}_k \rangle + \Omega \dot{E}_{0k} - \xi \dot{E}_{0k}\sum_q \dot{E}_{0q}\dot{E}_{0q}^* - \eta \dot{E}_{0k}^*\sum_q \dot{E}_{0q}\dot{E}_{0q}, \end{aligned} \tag{102}$$

where we introduced

$$\Omega = \phi(1-c)\Psi(\dot{\varepsilon}_2 - \dot{\varepsilon}_1) + \phi c \mathcal{M}(\dot{\varepsilon}_3 - \dot{\varepsilon}_1), \tag{103}$$

$$\xi = \phi(1-c)(\dot{\varepsilon}_2 - \dot{\varepsilon}_1)\mathcal{A}_t + \phi c \mathcal{A}_r, \tag{104}$$

$$\eta = \phi(1-c)(\dot{\varepsilon}_2 - \dot{\varepsilon}_1)\mathcal{B}_t + \phi c \mathcal{B}_r. \tag{105}$$

Similarly, the second balance equation for the electric field assumes the form

$$\begin{aligned} \langle \dot{E}_k \rangle &= \left[(1-\phi) + \phi(1-c)\Psi + \phi c \mathcal{M}\right]\dot{E}_{0k} \\ &\quad -\left[\phi(1-c)\mathcal{A}_t + \phi c \mathcal{A}\right]\dot{E}_{0k}\sum_q \dot{E}_{0q}\dot{E}_{0q}^* - \left[\phi(1-c)\mathcal{B}_t + \phi c \mathcal{B}\right]\dot{E}_{0k}^*\sum_q \dot{E}_{0q}\dot{E}_{0q} \\ &= = \Gamma \dot{E}_{0k} - \delta \dot{E}_{0k}\sum_q \dot{E}_{0q}\dot{E}_{0q}^* - \varrho \dot{E}_{0k}^*\sum_q \dot{E}_{0q}\dot{E}_{0q}, \end{aligned} \tag{106}$$

where, additionally, we defined

$$\Gamma = (1-\phi) + \phi(1-c)\Psi + \phi c\mathcal{M}, \tag{107}$$

$$\delta = \phi(1-c)\mathcal{A}_t + \phi c\mathcal{A}, \tag{108}$$

$$\varrho = \phi(1-c)\mathcal{B}_t + \phi c\mathcal{B}. \tag{109}$$

Now, to complete the homogenization procedure, we remember that the effective medium theory represents a constitutive equation combining $\langle \dot{D}_k \rangle$ with $\langle \dot{E}_k \rangle$. Therefore, to obtain such a relation we have to find $\dot{E}_{0k}$ in terms of $\langle \dot{E}_k \rangle$ from Eq. (106) and to substitute this result in Eq. (102). To begin, we invert Eq. (106), easily getting the expression

$$\dot{E}_{0k} = \frac{1}{\Gamma}\langle \dot{E}_k \rangle + \frac{\delta}{\Gamma^3\Gamma^*}\langle \dot{E}_k \rangle \sum_q \langle \dot{E}_q \rangle \langle \dot{E}_q^* \rangle + \frac{\varrho}{\Gamma^3\Gamma^*}\langle \dot{E}_k^* \rangle \sum_q \langle \dot{E}_q \rangle \langle \dot{E}_q \rangle. \tag{110}$$

Then, we substitute this result in Eq. (102) and, up to the third order in the electric field, we eventually obtain

$$\langle \dot{D}_k \rangle = \left(\dot{\varepsilon}_1 + \frac{\Omega}{\Gamma} \right) \langle \dot{E}_k \rangle + \frac{\delta\Omega - \xi\Gamma}{\Gamma^3\Gamma^*}\langle \dot{E}_k \rangle \sum_q \langle \dot{E}_q \rangle \langle \dot{E}_q^* \rangle + \frac{\varrho\Omega - \eta\Gamma}{\Gamma^3\Gamma^*}\langle \dot{E}_k^* \rangle \sum_q \langle \dot{E}_q \rangle \langle \dot{E}_q \rangle. \tag{111}$$

This represents the most important result of the present paper, fully characterizing the electrical response of the dispersion of composite particles with uniformly random orientations and positions. To conclude, we can also write down the effective parameters for the whole heterogeneous material as follows

$$\dot{\varepsilon}_{eff}(\omega) = \dot{\varepsilon}_1 + \frac{\Omega}{\Gamma}, \tag{112}$$

$$\dot{\chi}_{1,eff}(\omega) = \frac{2}{\Gamma^3\Gamma^*}(\delta\Omega - \xi\Gamma), \tag{113}$$

$$\dot{\chi}_{2,eff}(\omega) = \frac{4}{\Gamma^3\Gamma^*}(\varrho\Omega - \eta\Gamma). \tag{114}$$

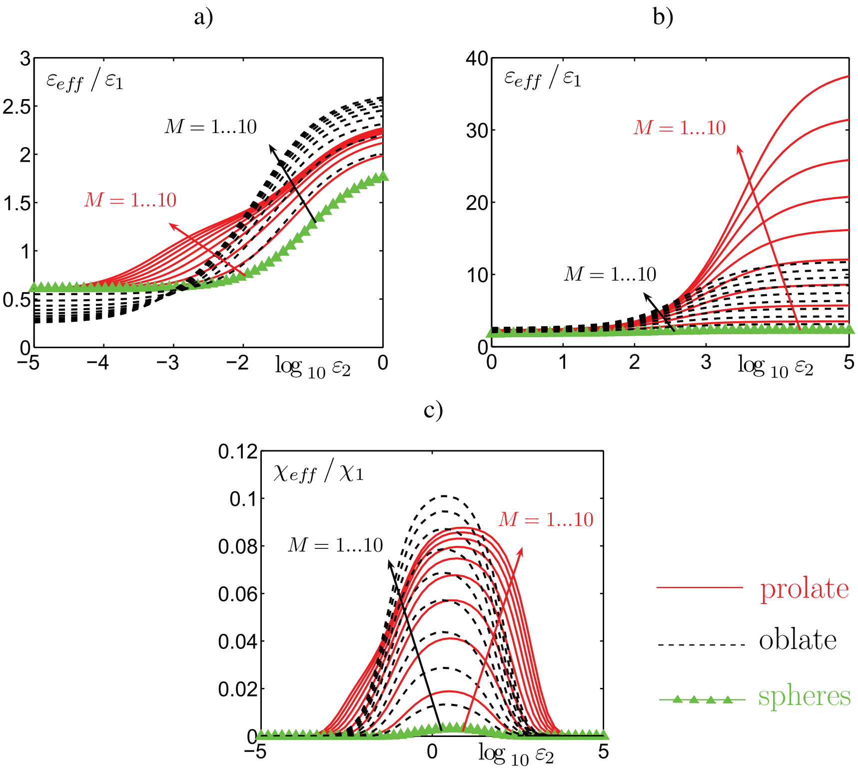

Fig. 4. Analysis of the effective parameters in the static case with the core-to matrix contrast $\varepsilon_3/\varepsilon_1 = 10$ ($\varepsilon_3 = 10$, $\varepsilon_1 = 1$). The overall response is shown versus $\log_{10}\varepsilon_2$ for prolate spheroids with axes $a_{s1} = 3M - 2$, $a_{s2} = 1$, $a_{s3} = 1$ (red continuous curves), spheres (green curves with triangles) and oblate spheroids with axes $a_{s1} = 1$, $a_{s2} = 1$, $a_{s3} = 1/(3M - 2)$ (black dashed curves). The results for the effective permittivity are split in two different ranges to improve the legibility. We fixed the volume fractions $c = 0.9$ and $\phi = 0.3$. (For interpretation of the references to colour in this figure legend, the reader is referred to the web version of this article.)

These results represent closed form expressions of the three effective quantities controlling the overall response of the heterogeneous material. We underline that the procedure can be easily implemented in a numerical code, useful to calculate the effective parameters at any frequency ω, as discussed in the next Section.

7. Numerical results

We start with a simple example concerning a purely static case, without temporal dispersion. It means that $\varepsilon_1, \varepsilon_2, \varepsilon_3$ and $\chi_1 = \chi_2$ assume real values, similarly to the results ε_{eff} and $\chi_{1,eff} = \chi_{2,eff}$. Indeed, in this static case it is easily proved that if $\chi_1 = \chi_2$, then we have $\chi_{1,eff} = \chi_{2,eff}$. This point can be analytically verified through Eqs. (113) and (114), combined with all the pertinent parameters. However, this is not always true, as discussed below for complex valued permittivities and nonlinear susceptibilities. We use the general theory to investigate the effect of the shell permittivity ε_2, the effect of the ellipsoidal particles shape and, finally, the effect of the core-to-matrix contrast $\varepsilon_3/\varepsilon_1$. The results are shown in Figs. 4–6, where the effective parameters have been represented in terms of the microstructure features. In particular, the three figures concern the contrast $\varepsilon_3/\varepsilon_1 = 10, 1, 0.1$, respectively. In all cases, we have used a volume fraction $c = 0.9$ for the core within each particle, and $\phi = 0.3$ for the entire population of composite particles. In each plot we have represented the results for prolate ellipsoids of revolution (spheroids of ovary or elongated form), spheres, and oblate ellipsoids of revolution (spheroids of planetary or flattened form). For representing the prolate shape we used three semiaxes defined as $a_{s1} = 3M - 2, a_{s2} = 1, a_{s3} = 1$, while for the oblate case we adopted $a_{s1} = 1, a_{s2} = 1, a_{s3} = 1/(3M - 2)$, where $M = 1 \dots 10$, to fully explore the effect of the shape on the overall response of the heterogeneous material. In both cases, $M = 1$ corresponds to the spherical shape. The above semiaxes definitions are coherent with the initial assumption $0 < a_{s,3} < a_{s,2} < a_{s,1} < +\infty$, stated in Section 3. In Figs. 4–6, results for prolate spheroids, spheres and oblate spheroids are represented by red, green and black curves, respectively. The results for the linear effective permittivity ε_{eff} have been reported, in each case, by means of two plots, the first in panel (a) showing $\varepsilon_{eff}/\varepsilon_1$ for $-5 < \log_{10}\varepsilon_2 < 0$, and the second in panel (b) showing $\varepsilon_{eff}/\varepsilon_1$ for $0 < \log_{10}\varepsilon_2 < 5$. This splitting permits to better observe the large modification of the linear results within the entire range of variation of $\log_{10}\varepsilon_2$. The limiting values of $\varepsilon_{eff}/\varepsilon_1$ for $\varepsilon_2 \to 0$ and $\varepsilon_2 \to \infty$ can be explained and checked as follows. For $\varepsilon_2 \to 0$, the system corresponds to a dispersion of voids (or better, zero permittivity particles) with volume fraction ϕ and, conversely, for $\varepsilon_2 \to \infty$ the system corresponds to a dispersion of metallic particles (superconducting particles if we deal

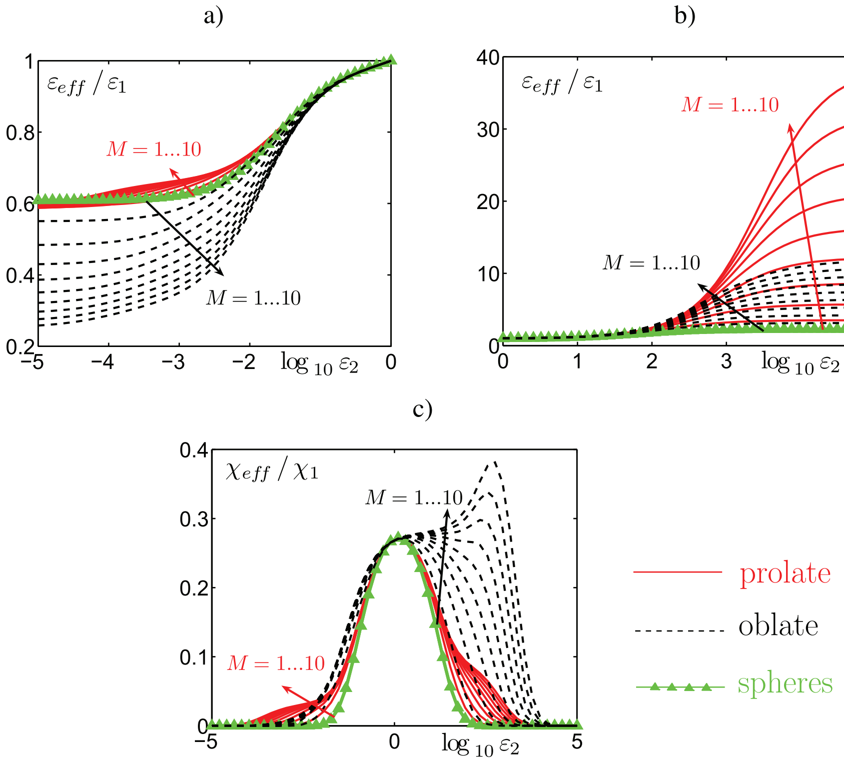

Fig. 5. Analysis of the effective parameters in the static case with the core-to matrix contrast $\varepsilon_3/\varepsilon_1 = 1$ ($\varepsilon_3 = \varepsilon_1 = 1$). The overall response is shown versus $\log_3\varepsilon_2$for prolate spheroids with axes $a_{s1} = 3M - 2, a_{s2} = 1, a_{s3} = 1$ (red continuous curves), spheres (green curves with triangles) and oblate spheroids with axes $a_{s1} = 1, a_{s2} = 1, a_{s3} = 1/(3M - 2)$ (black dashed curves). The results for the effective permittivity are split in two different ranges to improve the legibility. We fixed the volume fractions $c = 0.9$ and $\phi = 0.3$. (For interpretation of the references to colour in this figure legend, the reader is referred to the web version of this article.)

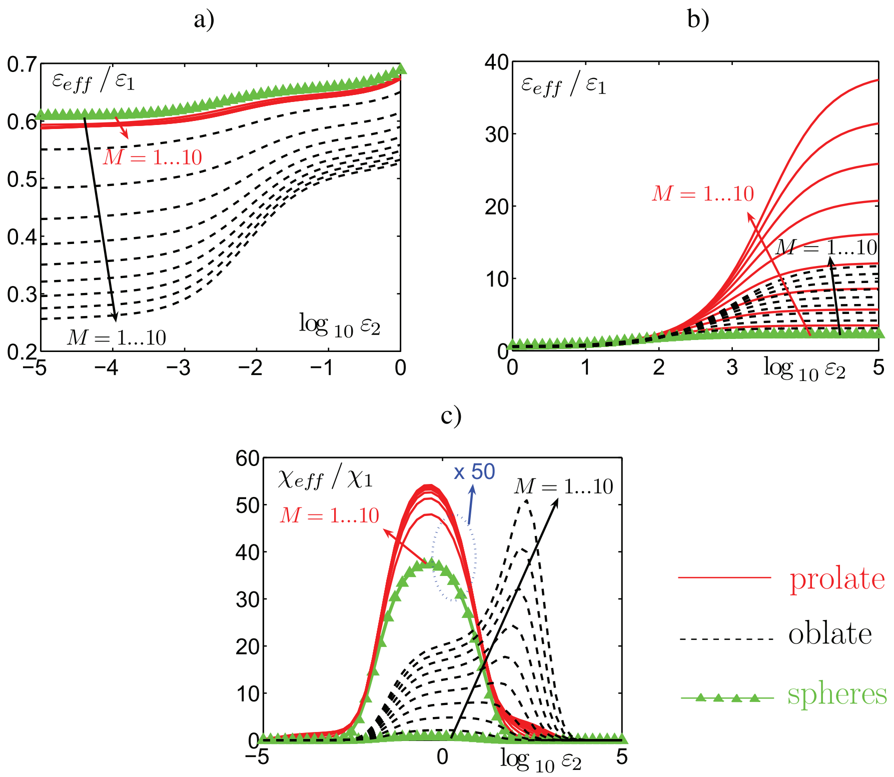

Fig. 6. Analysis of the effective parameters in the static case with the core-to matrix contrast $\varepsilon_3/\varepsilon_1 = 0.1$ ($\varepsilon_3 = 0.1$, $\varepsilon_1 = 1$). The overall response is shown versus $\log_{10}\varepsilon_2$for prolate spheroids with axes $a_{s1} = 3M - 2$, $a_{s2} = 1$, $a_{s3} = 1$ (red continuous curves), spheres (green curves with triangles) and oblate spheroids with axes $a_{s1} = 1$, $a_{s2} = 1$, $a_{s3} = 1/(3M - 2)$ (black dashed curves). The results for the effective permittivity are split in two different ranges to improve the legibility. We fixed the volume fractions $c = 0.9$ and $\phi = 0.3$. (For interpretation of the references to colour in this figure legend, the reader is referred to the web version of this article.)

with transport properties instead of dielectric ones) with the same volume fraction. In fact, because of the extremes values of the shell permittivity, the particle cores can not influence the effective properties. In the first case the electric induction can not enter the shell ($\vec{D}= 0$ since $\varepsilon_2 \to 0$), while in the second case is the electric field that can not penetrate the shell ($\vec{E}= 0$ since $\varepsilon_2 \to \infty$). Anyway, we can use the standard Maxwell–Garnett rule for the effective permittivity ε_{eff} of a dispersion of ellipsoids (ε_2) in a matrix (ε_1) with a volume fraction ϕ (Maxwell-Garnett, 1904; Fricke, 1953; Giordano, 2003)

$$\varepsilon_{eff} = \varepsilon_1 + \frac{\phi(\varepsilon_2 - \varepsilon_1)\frac{1}{3}\sum_j \frac{\varepsilon_1}{\varepsilon_1 + L_j(\varepsilon_2 - \varepsilon_1)}}{1 + \phi\left[\frac{1}{3}\sum_j \frac{\varepsilon_1}{\varepsilon_1 + L_j(\varepsilon_2 - \varepsilon_1)} - 1\right]}, \tag{115}$$

in order to examine the relevant limiting behaviors. If $\varepsilon_2 \to 0$, we obtain

$$\frac{\varepsilon_{eff}}{\varepsilon_1} = 1 - \frac{\phi\frac{1}{3}\sum_j \frac{1}{1-L_j}}{1 + \phi\left[\frac{1}{3}\sum_j \frac{1}{1-L_j} - 1\right]}, \tag{116}$$

while, for $\varepsilon_2 \to \infty$, we have

$$\frac{\varepsilon_{eff}}{\varepsilon_1} = 1 + \frac{\phi}{1-\phi}\frac{1}{3}\sum_j \frac{1}{L_j}. \tag{117}$$

We numerically proved that such limiting behaviors are in perfect agreement with results in Figs. 4–6, panels (a) and (b), for any shape of the involved ellipsoids, described by the pertinent depolarization factors. As regards the effective nonlinear response we presented the susceptibility χ_{eff} in panel (c), representing the values of $\chi_{1,eff} = \chi_{2,eff}$. We firstly observe that the limiting values $\lim_{\varepsilon_2=0}\chi_{eff} = \lim_{\varepsilon_2=\infty}\chi_{eff} = 0$ must be always fulfilled. Indeed, as above remarked, when $\varepsilon_2 \to 0$ or $\varepsilon_2 \to \infty$ the core does not affect the overall response of the heterogeneous material. Since the nonlinear character is solely contained in the particle cores, we must have a purely linear response when the core are not influencing the effective behavior (because of the shell shield). This behavior is correctly confirmed in Figs. 4–6, panel (c), for any value of the contrast

$\varepsilon_3/\varepsilon_1 = 10, 1, 0.1$. In all cases, χ_{eff}/χ_1 shows a maximum point for a specific value of the shell permittivity. Moreover, we observe that this peak is larger if $\varepsilon_3 < \varepsilon_1$ and if the particles are oblate. In Fig. 6, where $\varepsilon_3/\varepsilon_1 = 0.1$, we find a nonlinear response χ_{eff} as large as $50\chi_1$, for strongly oblate particle having $a_{s1} = 1, a_{s2} = 1, a_{s3} = 1/28$ ($M = 10$). We remark that in Fig. 6 the nonlinear responses for prolate particles, which are much weaker ($\chi_{eff} \simeq \chi_1$), have been represented with an intensification factor ($\times 50$) in order to facilitate the visualization. To conclude, we proved that, under specific conditions, we can obtain a large amplification of the nonlinear response, a phenomenon very useful to design composite materials with tailored nonlinear properties (an important point, e.g. in nonlinear optics).

In order to present a more complex example of application of the previous homogenization theory, we need to introduce a realistic behavior of a nonlinear material with temporal dispersion, to be used in the core of the composite particles. To do this we can develop a nonlinear version of the classical Drude–Lorentz model, largely used in optics (and nonlinear optics as well). The classical motion equation describing the dynamics of the position $\vec{r}$ of an electron elastically coupled to an atomic nucleous,

$$q\vec{E} - k\frac{d\vec{r}}{dt} - h\vec{r} - \beta(\vec{r}\cdot\vec{r})\vec{r} = m\frac{d^2\vec{r}}{dt^2}, \tag{118}$$

has been generalized with a third order term, controlled by the coefficient β, representing the anharmonicity of the coupling. In Eq. (118), $q\vec{E}$ is the Lorentz force applied to the electron charge q, k is the friction coefficient, h is the linear spring constant and m is the electron mass. Since we are interested in a sinusoidal steady state we can introduce the vector phasors for the electric field and the electron position. Hence, following the same procedure used in Section 2, the motion equation taking into account only the monochromatic terms at frequency ω assumes the form

$$\left[\left(\omega_0^2 - \omega^2\right) + i\omega\frac{k}{m}\right]\dot{\vec{r}} + \frac{\beta}{m}\left[\frac{1}{2}\left(\dot{\vec{r}}\cdot\dot{\vec{r}}^*\right)\dot{\vec{r}} + \frac{1}{4}\left(\dot{\vec{r}}\cdot\dot{\vec{r}}\right)\dot{\vec{r}}^*\right] = \frac{q}{m}\dot{\vec{E}}, \tag{119}$$

where we have introduced the resonance frequency $\omega_0 = \sqrt{h/m}$. This equation in $\dot{\vec{r}}$ can be solved up to the third order in the electric field. Then the polarization density vector can be obtained as $\dot{\vec{P}} = Nq\dot{\vec{r}}$, where N is the optical electrons density. The result is

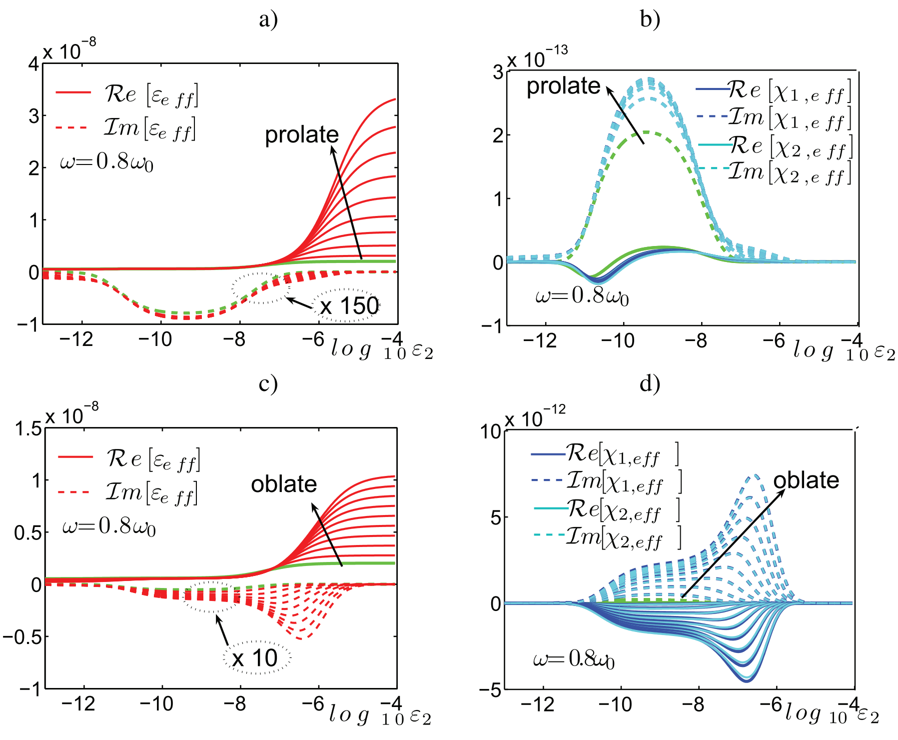

Fig. 7. Effective properties of the dispersion of composite particles with nonlinear dispersive cores described by Eqs. (121) and (122). Panels (a) and (b): linear and nonlinear results for prolate particles (axes $a_{s1} = 3M - 2, a_{s2} = 1, a_{s3} = 1$ with $M = 1\dots10$). Panel (c) and (d): linear and nonlinear results for oblate particles (axes $a_{s1} = 1, a_{s2} = 1, a_{s3} = 1/(3M - 2)$ with $M = 1\dots10$). In all plots continuous curves represent the real parts while dashed one the imaginary parts. Moreover, green curves concern the case with spherical particles. We considered a frequency $\omega = 0.8\omega_0$, before the resonance. We fixed $\varepsilon_1 = 100\varepsilon_0$, $c = 0.9$ and $\phi = 0.3$. (For interpretation of the references to colour in this figure legend, the reader is referred to the web version of this article.)

$$\dot{\vec{P}} = \frac{Nq^2}{m\left(\omega_0^2-\omega^2\right)+i\omega k}\dot{\vec{E}} - \frac{N\beta q^4\left[\frac{1}{2}\left(\dot{\vec{E}}\cdot\dot{\vec{E}}^*\right)\dot{\vec{E}}+\frac{1}{4}\left(\dot{\vec{E}}\cdot\dot{\vec{E}}\right)\dot{\vec{E}}^*\right]}{\left[m\left(\omega_0^2-\omega^2\right)+i\omega k\right]^2\left[m^2\left(\omega_0^2-\omega^2\right)^2+\omega^2k^2\right]}. \tag{120}$$

Finally, by considering the definition of the electric displacement vector $\dot{\vec{D}} = \varepsilon_0\dot{\vec{E}} + \dot{\vec{P}}$, we obtain a constitutive equation of the form given in Eq. (8) where $\chi_1(\omega) = \chi_2(\omega)$, i.e. a response as in Eq. (10), where

$$\dot{\varepsilon}_3(\omega) = \varepsilon_0 + \frac{Nq^2}{m\left(\omega_0^2-\omega^2\right)+i\omega k}, \tag{121}$$

$$\dot{\chi}_1(\omega) = -\frac{N\beta q^4}{\left[m\left(\omega_0^2-\omega^2\right)+i\omega k\right]^2\left[m^2\left(\omega_0^2-\omega^2\right)^2+\omega^2k^2\right]}. \tag{122}$$

In order to model the particles core we adopt the following parameters: $q = -1.6\times10^{-19}$ C, $m = 9.1\times10^{-31}$ Kg, $\varepsilon_0 = 8.85\times10^{-12}$ F/m, $\omega_0 = 100,000\ \mathrm{s}^{-1}$, $N = 3.1\times10^7\ \mathrm{m}^{-3}$, $k = 5\times10^{-26}$ Ns/m, $\beta = 1\times10^{-26}\ \mathrm{N/m}^3$ (arbitrary values used just to give an example of application of the theory). For the matrix we assume a fixed real permittivity $\varepsilon_1 = 100\varepsilon_0$ and for the shell a variable real permittivity $-13 < \log_{10}\varepsilon_2 < -4$. As before, we have used a volume fraction $c = 0.9$ for the core within each particle, and $\phi = 0.3$ for the entire population of composite particles. The results are shown in Figs. 7 and 8 in terms of $\log_{10}\varepsilon_2$, for two different frequencies $\omega = 0.8\omega_0$ and $\omega = 1.2\omega_0$, respectively. It means that we analyse the behavior of the system just before and after the resonance frequency ω_0. In both cases, we show in panels (a) and (b) the results for prolate particles and in panels (c) and (d) those for oblate particles. Moreover, in panels (a) and (c) we report the results for the real and imaginary part of the linear permittivity $\dot{\varepsilon}_{eff}$ and in panels (b) and (d) the real and imaginary part of the nonlinear susceptibilities $\dot{\chi}_{1,eff}$ and $\dot{\chi}_{2,eff}$. Firstly, we observe that, although $\dot{\chi}_1 = \dot{\chi}_2$ in the nonlinear Drude–Lorentz model, the mixing law previously obtained for the nonlinear response yields different values for $\dot{\chi}_{1,eff}$ and $\dot{\chi}_{2,eff}$ when the temporal dispersion is actually present. Nevertheless, the differences between $\dot{\chi}_{1,eff}$ and $\dot{\chi}_{2,eff}$ are quite negligible, as it can be seen in Figs. 7 and 8, panels (b) and (d). Therefore, also the whole system, when $\dot{\chi}_1 = \dot{\chi}_2$, can be approximately described with a constitutive equation as in Eq. (10). We further observe that the limiting values $\lim_{\varepsilon_2=0}\dot{\chi}_{eff} = \lim_{\varepsilon_2=\infty}\dot{\chi}_{eff} = 0$ are always fulfilled also in this

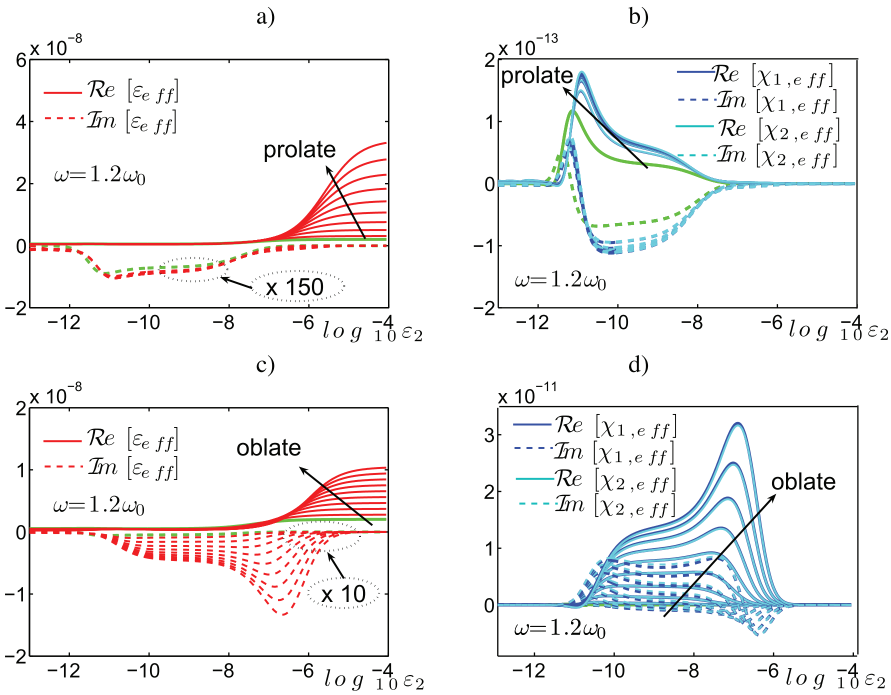

Fig. 8. Linear and nonlinear effective properties of the dispersion of composite particles with nonlinear dispersive cores described by Eqs. (121) and (122). Panels (a) and (b): linear and nonlinear results for prolate particles (axes $a_{s1} = 3M - 2$, $a_{s2} = 1$, $a_{s3} = 1$ with $M = 1\ldots10$). Panel (c) and (d): linear and nonlinear results for oblate particles (axes $a_{s1} = 1$, $a_{s2} = 1$, $a_{s3} = 1/(3M-2)$ with $M = 1\ldots10$). In all plots continuous curves represent the real parts while dashed one the imaginary parts. Moreover, green curves concern the case with spherical particles. We considered a frequency $\omega = 1.2\omega_0$, after the resonance. We fixed $\varepsilon_1 = 100\varepsilon_0$, $c = 0.9$ and $\phi = 0.3$. (For interpretation of the references to colour in this figure legend, the reader is referred to the web version of this article.)

case with dispersion, as expected. Finally, we remark that the amplification of the nonlinear properties when $|\dot{\varepsilon}_3| < \varepsilon_1$ is again observed for oblate particles, as clearly visible in panel (d) of Figs. 7 and 8.

8. Conclusions

In this work, we considered the problem of homogenizing a population of randomly oriented coated ellipsoidal particles from the dielectric point of view. We supposed to deal with linear responses for matrix and shells, while the cores have been considered with a nonlinear behavior, expanded up to the third order in the electric field. Moreover, all constitutive equations exhibit hereditary phenomena (the-so-called temporal dispersion). The problems introduced by such memory effects can be handled by working in the Fourier domain, useful to describe a sinusoidal steady-state at a given frequency ω. On the other hand, the difficulties generated by the nonlinear behaviors have been overcome by proving that the electric field within the cores remain uniform independently of their constitutive equations. Then, its value has been determined by solving an implicit equation based on a frequency and field dependent permittivity tensor. Performing the averaging over the orientations and over the heterogeneous material volume, we elaborated an effective medium theory, allowing the calculation of the linear and nonlinear overall response. The originality of this procedure resides in the fact that we have combined (i) the randomness of the orientations, (ii) the presence of an inter-phase between cores and matrix and, finally, (iii) the linear and nonlinear hereditary response of the constituents.

Appendix A. A property of the normal unit vector to an ellipsoidal surface

We consider an ellipsoids with axes a_1, a_2 and a_3 described by the parametric representation $x_1 = a_1 \sin\vartheta \cos\varphi, x_2 = a_2 \sin\vartheta \sin\varphi$ and $x_3 = a_3 \cos\vartheta$, where $0 < \varphi < 2\pi$ and $0 < \vartheta < \pi$. This representation can be written in compact form as $\vec{r} = \vec{r}(\vartheta, \varphi)$ where $\vec{r} = (x_1, x_2, x_3)$ is the position vector. Therefore, the normal unit vector may be calculated through the standard expression

$$\vec{n} = \frac{\frac{\partial \vec{r}}{\partial \vartheta} \wedge \frac{\partial \vec{r}}{\partial \varphi}}{\left|\left| \frac{\partial \vec{r}}{\partial \vartheta} \wedge \frac{\partial \vec{r}}{\partial \varphi} \right|\right|}. \tag{A.1}$$

Performing the calculation we obtain

$$\vec{n} = \frac{1}{\mathcal{N}}\left(a_2 a_3 \sin^2\vartheta \cos\varphi, a_1 a_3 \sin^2\vartheta \sin\varphi, a_1 a_2 \sin\vartheta \cos\vartheta\right), \tag{A.2}$$

where $\mathcal{N}$ is given by

$$\mathcal{N} = \sqrt{a_2^2 a_3^2 \sin^4\vartheta \cos^2\varphi + a_1^2 a_3^2 \sin^4\vartheta \sin^2\varphi + a_1^2 a_2^2 \sin^2\vartheta \cos^2\vartheta}. \tag{A.3}$$

Now, it is not difficult to develop the following two expressions

$$\sum_{j=1}^{3} \frac{x_j^2}{a_j^4} = \frac{\mathcal{N}^2}{\sin^2\vartheta\, a_1^2 a_2^2 a_3^2}, \qquad \sum_{j=1}^{3} \frac{x_j n_j}{a_j^2} = \frac{\mathcal{N}}{\sin\vartheta\, a_1 a_2 a_3}, \tag{A.4}$$

where we have used Eq. (A.2) and the parametric representation of the ellipsoidal surface. The ratio between previous quantities is therefore given by

$$\left(\sum_{j=1}^{3} \frac{x_j n_j}{a_j^2}\right) \Bigg/ \left(\sum_{j=1}^{3} \frac{x_j^2}{a_j^4}\right) = \frac{\sin\vartheta\, a_1 a_2 a_3}{\mathcal{N}}. \tag{A.5}$$

Now, since we can easily verify that $\sin\vartheta\, a_1 a_2 a_3 / \mathcal{N} = n_k a_k^2 / x_k$, $\forall k$, we finally obtain the interesting property

$$n_k = \frac{x_k}{a_k^2} \sum_j \frac{x_j n_j}{a_j^2} \Bigg/ \sum_j \frac{x_j^2}{a_j^4} \quad (\forall\ k = 1, 2, 3), \tag{A.6}$$

which is valid for any point belonging to the ellipsoidal surface. This result has been exploited in Eqs. (34) and (38), for the core–shell interface and for the shell-matrix interface, respectively.

References

Andrews, S. S. (2004). Using rotational averaging to calculate the bulk response of isotropic and anisotropic samples from molecular parameters. *Journal of Chemical Education, 81*, 877–885.

Benveniste, Y., & Miloh, T. (1986). The effective conductivity of composites with imperfect thermal contact at constituent interfaces. *International Journal of Engineering Science, 24*, 1537.

Benveniste, Y. (1987). Effective thermal conductivity of composites with a thermal contact resistance between the constituents: Nondilute case. *Journal of Applied Physics, 61*, 2840.

Benveniste, Y., & Miloh, T. (1991). On the effective thermal conductivity of coated short-fiber composites. *Journal of Applied Physics, 69*, 1337.

Benveniste, Y. (2013). Models of thin interphases and the effective medium approximation in composite media with curvilinearly anisotropic coated inclusions. *International Journal of Engineering Science, 72*, 140.

Bergman, D. J., Levy, O., & Stroud, D. (1994). Theory of optical bistability in a weakly nonlinear composite medium. *Physical Review B, 49*, 129.

Boyd, R. W. (2008). *Nonlinear optics*. New York: Academic Press.

Bruggeman, D. A. G. (1935). Dielektrizitatskonstanten und Leitfahigkeiten der Mishkorper aus isotropen Substanzen. *Annalen der Physik (Leipzig), 24*, 636.

Colombo, L., & Giordano, S. (2011). Nonlinear elasticity in nanostructured materials. *Report on Progress in Physics, 74*, 116501.

Duan, H. L., & Karihaloo, B. L. (2007). Effective thermal conductivities of heterogeneous media containing multiple imperfectly bonded inclusions. *Physical Review B, 75*, 064206.

Eshelby, J. D. (1957). The determination of the elastic field of an ellipsoidal inclusion, and related problems. *Proceedings of the Royal Society of London, A241*, 376–396.

Fricke, H. (1953). The Maxwell–Wagner dispersion in a suspension of ellipsoids. *Journal of Physical Chemistry, 57*, 934.

Furtado, L. A., de, M., & Gómez-Malagón, L. A. (2014). Simulation of the linear and nonlinear optical properties of colloids containing metallic core-dielectric shell nanoellipsoids. *Plasmonics, 9,*, 1377–1389.

Giordano, S. (2003). Effective medium theory for dispersions of dielectric ellipsoids. *Journal of Electrostatics, 58*, 59.

Giordano, S. (2005). Multipole analysis of a generic system of dielectric cylinders and application to fibrous materials. *Journal of Electrostatics, 63*, 1.

Giordano, S. (2005). Order and disorder in heterogeneous material microstructure: electric and elastic characterization of dispersions of pseudo oriented spheroids. *International Journal of Engineering Science, 43*, 1033–1058.

Giordano, S., & Rocchia, W. (2005). Shape dependent effects of dielectrically nonlinear inclusions in heterogeneous media. *Journal of Applied Physics, 98*, 104101.

Giordano, S., & Rocchia, W. (2006). Predicting dielectric nonlinearity of anisotropic composite materials via tensorial analysis. *Journal of Physics: Condensed Matter, 18*, 10585.

Giordano, S. (2007). Relation Between Microscopic and Macroscopic Mechanical Properties in Random Mixtures of Elastic Media. *Journal of Engineering Materials and Technology, 129*, 453–461.

Giordano, S., & Colombo, L. (2007). Effects of the orientational distribution of cracks in isotropic solids. *Engineering Fracture Mechanics, 74*, 1983–2003.

Giordano, S., & Palla, P. L. (2008). Dielectric behavior of anisotropic inhomogeneities: Interior and exterior points Eshelby tensors. *Journal of Physics A: Mathematical and Theoretical, 41*, 415205.

Giordano, S., Palla, P. L., & Colombo, L. (2008). Effective permittivity of materials containing graded ellipsoidal inclusions. *European Physical Journal B, 66*, 29.

Giordano, S., & Palla, P. L. (2012). Conduction degradation in anisotropic multi-cracked materials. *European Physical Journal B, 85*, 59.

Giordano, S. (2014). Explicit nonlinear homogenization for magneto-electro-elastic laminated materials. *Mechanics Research Communications, 55*, 18–29.

Giordano, S., Goueygou, M., Tiercelin, N., Talbi, A., Pernod, P., & Preobrazhensky, V. (2014). Magneto-electro-elastic effective properties of multilayered artificial multiferroics with arbitrary lamination direction. *International Journal of Engineering Science, 78*, 134–153.

Giordano, S., & Manca, F. (2014). Analysis of heterogeneous structures described by the two-temperature model. *International Journal of Heat and Mass Transfer, 78*, 189–202.

Goncharenko, A. V., Popelnukh, V. V., & Venger, E. F. (2002). Effect of weak nonsphericity on linear and nonlinear optical properties of small particle composites. *Journal of Physics D: Applied Physics, 35*, 1833–1838.

Goncharenko, A. V. (2004). Optical properties of core-shell particle composites. *I. Linear response. Chemical Physics Letters, 386*, 25–31.

Goncharenko, A. V. (2007). Optical properties of core-shell particle composites. II. Nonlinear response. *Chemical Physics Letters, 439*, 121–126.

Guerder, P.-Y., Giordano, S., Bou Matar, O., & Vasseur, J. O. (2015). Tuning the elastic nonlinearities in composite nanomaterials. *Journal of Physics: Condensed Matter, 27*, 145304.

Günther, R., & Heinrich, D. (1965). Dielektrizitätskonstante, Permeabilität, elektrische Leitfähigkeit, Wärmeleitfähigkeit und Diffusionskonstante von Gemischen mit kugelförmigen Teilchen (gitterförmige und statistische Anordnung). *Zeitschrift für Physik, 185*, 345.

Hashin, Z. (2001). Thin interphase/imperfect interface in conductivity. *Journal of Applied Physics, 89*, 2261.

Hasselman, D. P. H., & Johnson, L. F. (1987). Effective thermal conductivity of composites with interfacial thermal barrier resistance. *Journal Composite Materials, 21*, 508.

Hatta, H., & Taya, M. (1985). Effective thermal conductivity of a misoriented short fiber composite. *Journal of Applied Physics, 58*, 2478.

Hatta, H., & Taya, M. (1986). Equivalent inclusion method for steady state heat conduction in composites. *International Journal of Engineering Science, 24*, 1159.

Hatta, H., & Taya, M. (1986). Thermal conductivity of coated filler composites. *Journal of Applied Physics, 59*, 1851.

Hui, P. M., Cheung, P., & Stroud, D. (1998). Theory of third harmonic generation in random composites of nonlinear dielectric. *Journal of Applied Physics, 84*, 3451.

Kachanov, M. (1994). Elastic solids with many cracks and related problems. *Advanced Applied Mechanics, 30*, 259–445.

Kachanov, M., & Sevostianov, I. (2005). On quantitative characterization of microstructures and effective properties. *International Journal of Solids and Structures, 42*, 309–336.

Kanaun, S., & Levin, V. (2008a). Self-consistent methods for composites. *Static problems*: Vol. 1. Dordrecht: Springer.

Kanaun, S., & Levin, V. (2008b). Self-consistent methods for composites. *Wave propagation in heterogeneous materials*: Vol. 2. Dordrecht: Springer.

Kanaun, S., & Levin, V. (2009). Elliptical cracks arbitrarily oriented in 3D-anisotropic elastic media. *International Journal of Engineering Science, 47*, 777–792.

Kanaun, S. (2010). On the effective elastic properties of matrix composites: Combining the effective field method and numerical solutions for cell elements with multiple inhomogeneities. *International Journal of Engineering Science, 48*, 160–173.

Kanaun, S. (2011). Calculation of electro and thermo static fields in matrix composite materials of regular or random microstructures. *International Journal of Engineering Sciences, 49*, 41–60.

Kanaun, S., & Markov, A. (2014). Stress fields in 3D-elastic material containing multiple interacting cracks of arbitrary shapes: Efficient calculation. *International Journal of Engineering Science, 75*, 118–134.

Kapitza, P. L. (1964). *Collected papers of P.L. Kapitza*: Vol. 3. Oxford: Pergamon Press.

Kauranen, M., & Zayats, A. V. (2012). Nonlinear plasmonics. *Nature Photonics, 6*, 737–748.

Kim, J. Y. (2011). Micromechanical analysis of effective properties of magneto-electro-thermo-elastic multilayer composites. *International Journal of Engineering Science, 49*, 1001–1018.

Kröner, E. (1978). Self-consistent scheme and graded disorder in polycrystal elasticity. *Journal of Physics F: Metal Physics, 8*, 2261–2267.

Kushch, V. I., Sevostianov, I., & Belyaev, A. S. (2015). Effective conductivity of spheroidal particle composite with imperfect interfaces: Complete solutions for periodic and random micro structures. *Mechanics of Materials, 89*, 1.

Lakhtakia, A., & Weiglhofer, W. S. (2000). Maxwell-Garnett formalism for weakly nonlinear, bianisotropic, dilute, particulate composite media. *International Journal of Electronics, 87*, 1401.

Landau, L. D., Pitaevskii, L. P., & Lifshitz, E. M. (1984). *Electrodynamics of continuous media*. Oxford: Butterworths Heinemann.

Lapine, M., Shadrivov, I. V., & Kivshar, Y. S. (2014). Colloquium: Nonlinear metamaterials. *Reviews of Modern Physics, 86*, 1093.

Le Quang, H., Bonnet, G., & He, Q.-C. (2010). Size-dependent Eshelby tensor fields and effective conductivity of composites made of anisotropic phases with highly conducting imperfect interfaces. *Physical Review B, 81*, 064203.

Le Quang, H., He, Q.-C., & Bonnet, G. (2011). Eshelby's tensor fields and effective conductivity of composites made of anisotropic phases with Kapitza's interface thermal resistance. *Philosophical Magazine, 91*, 3358.

Le Quang, H., Pham, D. C., Bonnet, G., & He, Q.-C. (2013). Estimations of the effective conductivity of anisotropic multiphase composites with imperfect interfaces. *International Journal of Heat and Mass Transfer, 58*, 175.
Lipton, R., & Vernescu, B. (1996). Critical radius, size effects and extremal microgeometries for composites with imperfect interface. *Journal of Applied Physics, 79*, 8964.
Lipton, R. (1997). Variational methods, bounds, and size effects for composites with highly conducting interface. *Journal of Mechanics and Physics of Solids, 45*, 361.
Mackay, T. G. (2011). Effective constitutive parameters of linear nanocomposites in the long-wavelength regime. *Journal of Nanophotonics, 5*, 051001.
Markov, M., Levin, V., Mousatov, A., & Kazatchenko, E. (2012). Generalized DEM model for the effective conductivity of a two-dimensional percolating medium. *International Journal of Engineering Science, 58*, 78–84.
Markov, M., Mousatov, A., Kazatchenko, E., & Markova, I. (2014). Determination of electrical conductivity of double-porosity formations by using generalized differential effective medium approximation. *Journal of Applied Geophysics, 108*, 104–109.
Maxwell, J. C. (1881). *A Treatise on Electricity and Magnetism*. Oxford: Clarendon.
Maxwell-Garnett, J. C. (1904). Colours in metal glasses and in metallic films. In *Philosophical transactions of the royal society of london*, Ser. A, 203, 385.
Meredith, R. E. (1959). Studies on the conductivities of dispersions. Lawrence Radiation Laboratory (Berkeley, California), Report No. UCRL-8667.
Mills, D. L. (1991). *Nonlinear optics*. Berlin: Springer-Verlag.
Miloh, T., & Benveniste, Y. (1999). On the effective conductivity of composites with ellipsoidal inhomogeneities and highly conducting interfaces. *Proceedings of the Royal Society of London, A455*, 2687.
Milton, G. W. (2004). *The theory of composites*. Cambridge: Cambridge University Press.
Myles, T. M., Peracchio, A. A., & Chiu, W. K. S. (2014). Effect of orientation anisotropy on calculating effective electrical conductivities. *Journal of Applied Physics, 115*, 203503.
Myles, T. M., Peracchio, A. A., & Chiu, W. K. S. (2015). Extension of anisotropic effective medium theory to account for an arbitrary number of inclusion types. *Journal of Applied Physics, 117*, 025101.
Nan, C.-W., Birringer, R., Clarke, D. R., & Gleiter, H. (1997). Effective thermal conductivity of particulate composites with interfacial thermal resistance. *Journal of Applied Physics, 81*, 6692.
Norris, A. N. (1985). A differential scheme for the effective moduli of composites. *Mechanics of Materials, 4*, 1–16.
Pavanello, F., Manca, F., Palla, P. L., & Giordano, S. (2012). Generalized interface models for transport phenomena: Unusual scale effects in composite nanomaterials. *Journal of Applied Physics, 112*, 084306.
Pavanello, F., & Giordano, S. (2013). How imperfect interfaces affect the nonlinear transport properties in composite nanomaterials. *Journal of Applied Physics, 113*, 154310.
Pinchuk, A. (2003). Optical bistability in nonlinear composites with coated ellipsoidal nanoparticles. *Journal of Physics D: Applied Physics, 36*, 460–464.
Sahimi, M. (2003). *Heterogeneous materials I, linear transport and optical properties*. New York: Springer-Verlag.
Sahimi, M. (2003). *Heterogeneous materials II, nonlinear and breakdown properties and atomistic modeling*. New York: Springer-Verlag.
Sihvola, A. (1999). *Electromagnetic mixing formulas and applications*. London: The Institution of Electrical Engineers.
Tartar, L. (2009). *The general theory of homogenization: A personalized introduction*. Berlin: Springer-Verlag.
Torquato, S., & Rintoul, M. D. (1995). Effect of the interface on the properties of composite media. *Physical Review Letters, 75*, 4067.
Torquato, S. (2002). *Random heterogeneous materials: Microstructure and macroscopic properties*. New York: Springer-Verlag.
van Beek, L. K. H. (1967). Dielectric behavior of heterogeneous systems. *Progress in Dielectrics, 7*, 71.
Weiglhofer, W. S., Lakhtakia, A., & Michel, B. (1997). Maxwell-Garnett and Bruggeman formalisms for a particulate composite with bianisotropic host medium. *Microwave and Optical Technology Letters, 15*, 263.
Xu, W., Chen, H., Chen, W., & Jiang, L. (2014). Prediction of transport behaviors of particulate composites considering microstructures of soft interfacial layers around ellipsoidal aggregate particles. *Soft Matter, 10*, 627–638.